TECHNICAL MEMORANDUM

Geomorphic and Two-Dimensional Hydraulic Modeling Evaluation of the Little Miami River in the Eastern Corridor Segment II/III Study Area - Phase One Report

PREPARED FOR: Deborah Osborne / Entran

PREPARED BY: Mark Tompkins/ CH2M HILL
Anthony Falzone/ CH2M HILL
Kyle Winslow/ CH2M HILL

DATE: March 2, 2009

Table of Contents

1 Introduction and Purpose

The purpose of the Eastern Corridor investments as documented in the Tier 1 Record Of Decision (ROD) is to implement a multimodal transportation program that increases capacity, reduces congestion and delay, improves safety, provides transportation options, and connects the region's key transportation corridors and social and economic centers by the efficient movement of people, goods, and services. The specific goal for Segment II/III, in support of the overall purpose and need for the Eastern Corridor Multimodal program, is to establish relocated SR 32 as a controlled access arterial roadway west of I-275, with parallel rail transit. SR 32 in the Segment II/III area is a mostly developed commercial/industrial and residential corridor that experiences high volumes of commuter, freight and residential traffic. The need for transportation improvements results from insufficient levels-of-service and high crash rates that are currently being experienced along existing SR 32 and are expected to worsen by 2030 (the project design year).

Segment II/III of the Eastern Corridor will include one crossing of the Wild and Scenic designated Little Miami River in the general vicinity of "Horseshoe Bend," an extreme meander in the river's course (Figures 1 and 2). This technical memorandum summarizes the geomorphic setting, watershed hydrology, historical channel evolution, and hydraulic characteristics of the Study Area developed through detailed investigations of site specific hydrology, geomorphology, and hydraulics conducted to evaluate the long-term stability of the Little Miami River. The findings from these analyses will be considered in the Conceptual Alternatives Study (CAS) to assist in the identification of feasible alternatives to be advanced for further study.

The analyses summarized in this document were conducted in parallel with a Rosgen-type river morphology investigation to provide a comprehensive, complementary, and defensible approach to this complex issue. Both studies are being conducted in two phases, and focus on a 2.5 mile section of the Little Miami River near the Horseshoe Bend (approximately river mile 4.5 to river mile 7.0) (Figure 2). The goal of the first phase analyses summarized in this document was to identify specific reaches within the 2.5 mile Study Area that exhibit preferable stability characteristics based on local hydraulics, sediment transport, and geomorphic characteristics. The results of this initial "feasibility" phase will be considered in the CAS evaluation and the advancement of feasibility alternatives for further study. A second phase of this evaluation will focus on validating predictive assumptions and identifying implications for channel morphology and stability in the project area.

2 Geomorphic Setting

General geomorphic conditions in the Study Area are summarized here based on regional geology data from H.C. Nutting (2008), channel sediment sampling data from Stantec (2008), and general observations by CH2M HILL's senior fluvial geomorphologist during reconnaissance of the Study Area on September 8 and 9, 2008. The Little Miami River watershed encompasses approximately 1,758 square miles in the southwestern corner of Ohio (Figure 1). The headwaters are located near Springfield, Ohio, and the confluence with

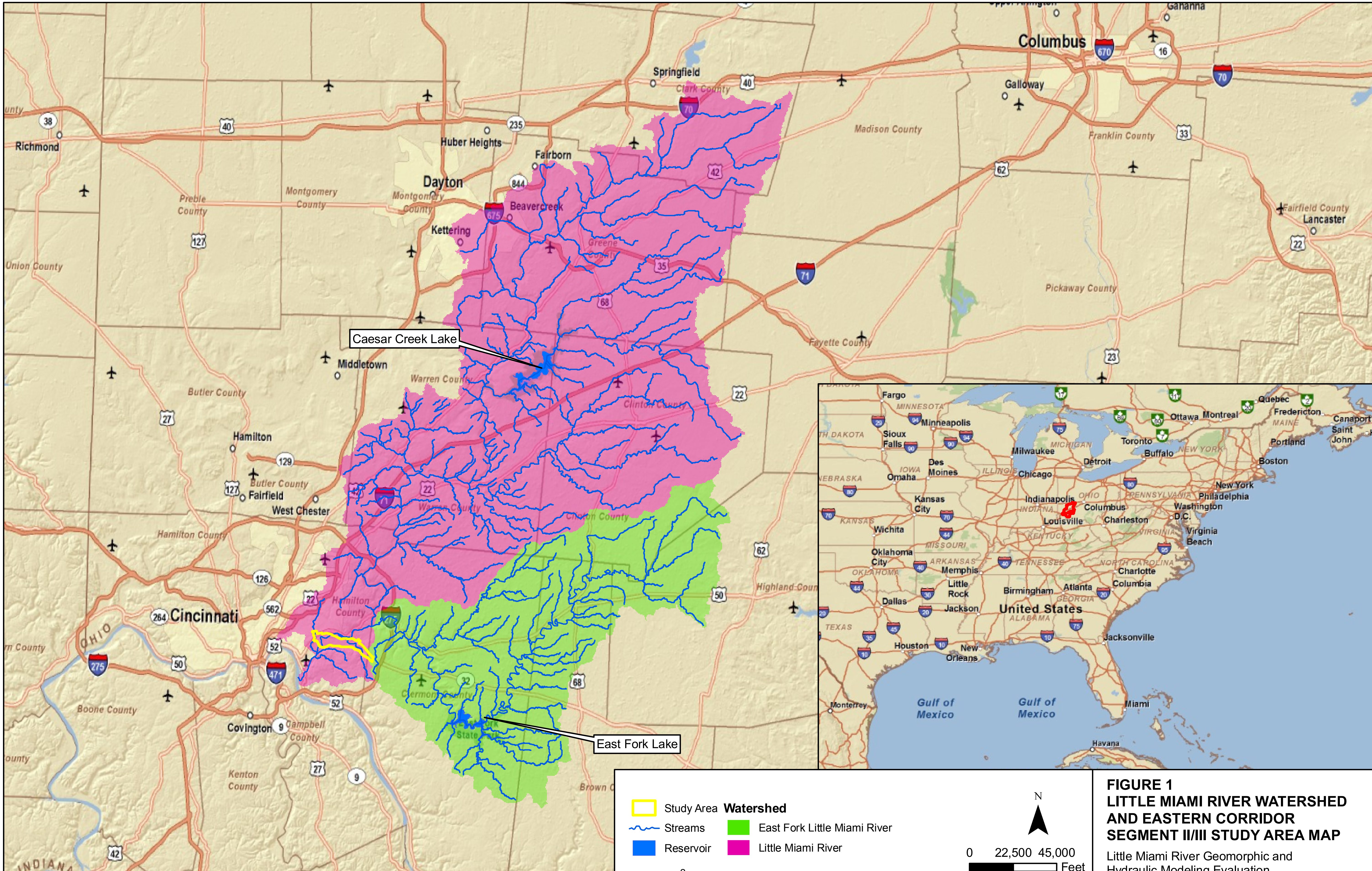

FIGURE 1
LITTLE MIAMI RIVER WATERSHED AND EASTERN CORRIDOR SEGMENT II/III STUDY AREA MAP
Little Miami River Geomorphic and Hydraulic Modeling Evaluation

\\SFO31029951\PROJECTS\LITTLEMIAMIRIVER\GIS\MAPFILES\WATERSHEDMAP.MXD WATERSHEDMAP.MXD AFALZONE 1/23/2009 13:56:11

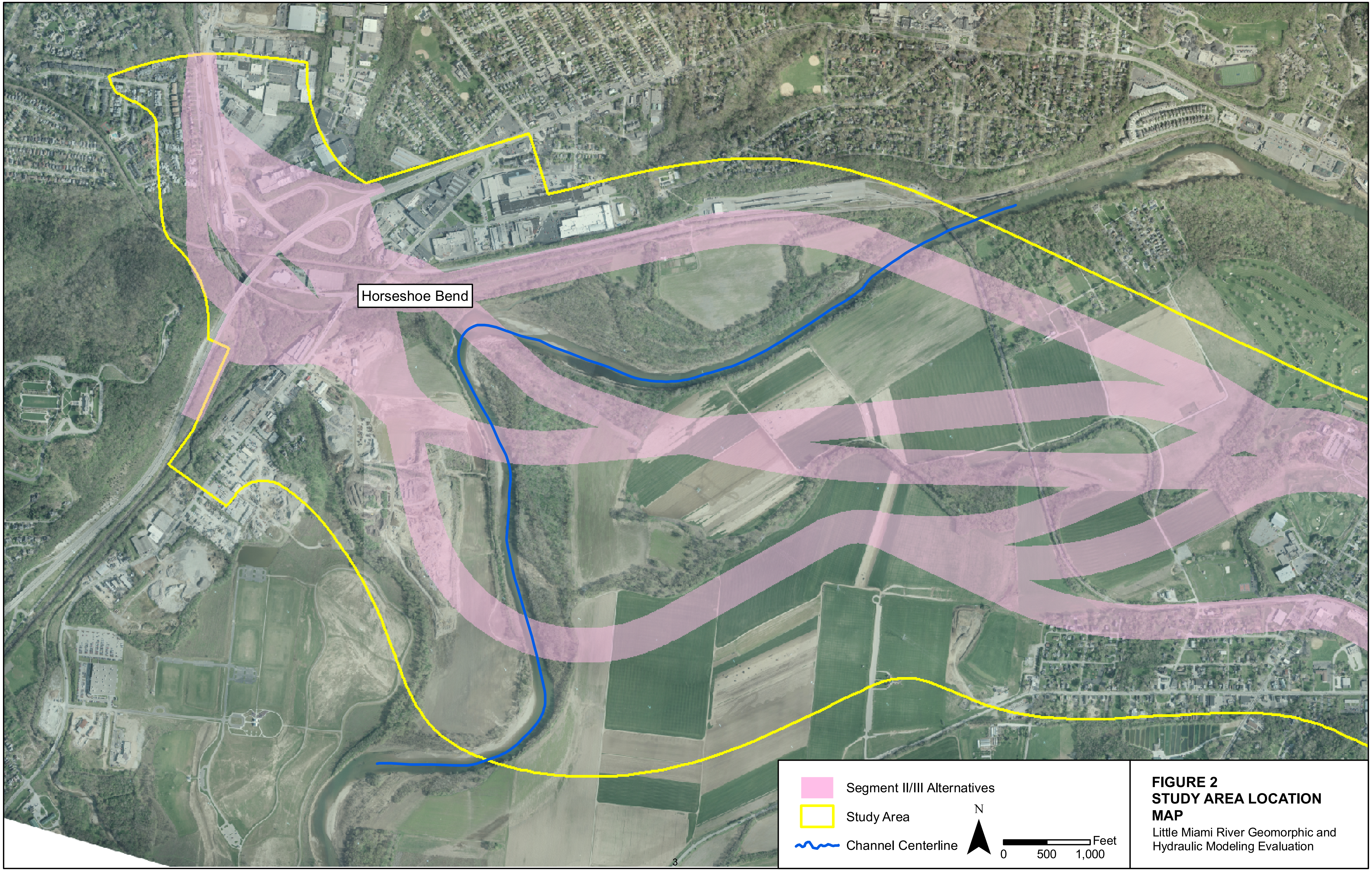

FIGURE 2
STUDY AREA LOCATION MAP
Little Miami River Geomorphic and Hydraulic Modeling Evaluation

\\SFO31029951\PROJECTS\LITTLEMIAMIRIVER\GIS\MAPFILES\STUDYSITELOCMAPZOOMEDIN.MXD STUDYSITELOCMAPZOOMEDIN.MXD AFALZONE 1/23/2009 14:01:54

the Ohio River is approximately seven miles upstream of Cincinnati (Schiefer 2002). The modern Little Miami River is incised into a glacially influenced floodplain in the Study Area. This floodplain is composed of fine silts and sands deposited when glaciers blocked the course of the Ohio River and created proglacial lakes in the Little Miami River valley. The glacial origin of floodplain sediments in the Study Area is consistent with channel bank sediment samples (Figure 3) that are dominated by fine sand, silt, and clay.

The stratigraphy of floodplain deposits in the Study Area illustrates both the fluvial and glacial nature of sediment deposition in the Little Miami River valley. Currently, the uppermost zone is typically covered by a sandy alluvium that grades into silts and clays deposited by large floods on the Ohio River and its tributaries (including the Little Miami River). Below the upper alluvial layer, the soil column exhibits complex layering between sand and gravel with minor fines, thick sequences of glacial outwash and valley train deposits, and lacustrine deposits. Groundwater depths in the Study Area are generally dependent on the stage of the Ohio River. As is typical of lowland rivers in fine-grained valley deposits, high flows in the Little Miami River have actively worked and reworked the floodplain since the last period of glaciation.

The Little Miami River itself is a dynamic, meandering channel that reflects both the hydrology of its watershed and the fine-grained sediment that composes the river's floodplain. There are currently several active mid-channel bars and point bars in the Study Area. Pebble counts collected on bars throughout the Study Area (Figure 3) show that the surface layers of these bars generally fine in the downstream direction and have median particle diameters as large as 45 mm near their upstream ends and as large as 22.6 mm near their downstream ends. Bulk samples conducted on these bars (Figure 3) show that the subsurface composition of the bars also reflects regular channel bed mobilization, with median particle diameters that are consistently finer (between 5 mm and 27 mm) than the surface layer of the bar. This bar morphology, combined with the presence of riparian vegetation assemblages with diverse age structures, is indicative of the dynamic nature of the bar features and the channel in general.

The geomorphic history and current conditions in the Study Area highlight the importance of careful consideration of geomorphic processes and long-term channel change in the site selection for and design of a clear span bridge crossing over the Little Miami River. The relatively large mobile bed material indicates that the Little Miami River is a high energy system during peak discharges. The effects of this high energy can be seen throughout the Study Area where the root networks of mature trees have been exposed and where adjacent land has been protected by riprap or other channel armoring. Appendix A includes a selection of annotated photographs illustrating the dynamic nature of the Little Miami River in the Study Area.

3 Hydrologic Analyses

An understanding of historical, current, and likely future hydrologic patterns is useful in interpreting past changes in channel morphology and expected future channel evolution. In addition, historical and current hydrology information is required as an input parameter for the hydraulic modeling component of this evaluation. The Eastern Corridor Segment II/III Study Area is located approximately six miles downstream of the confluence of the Little

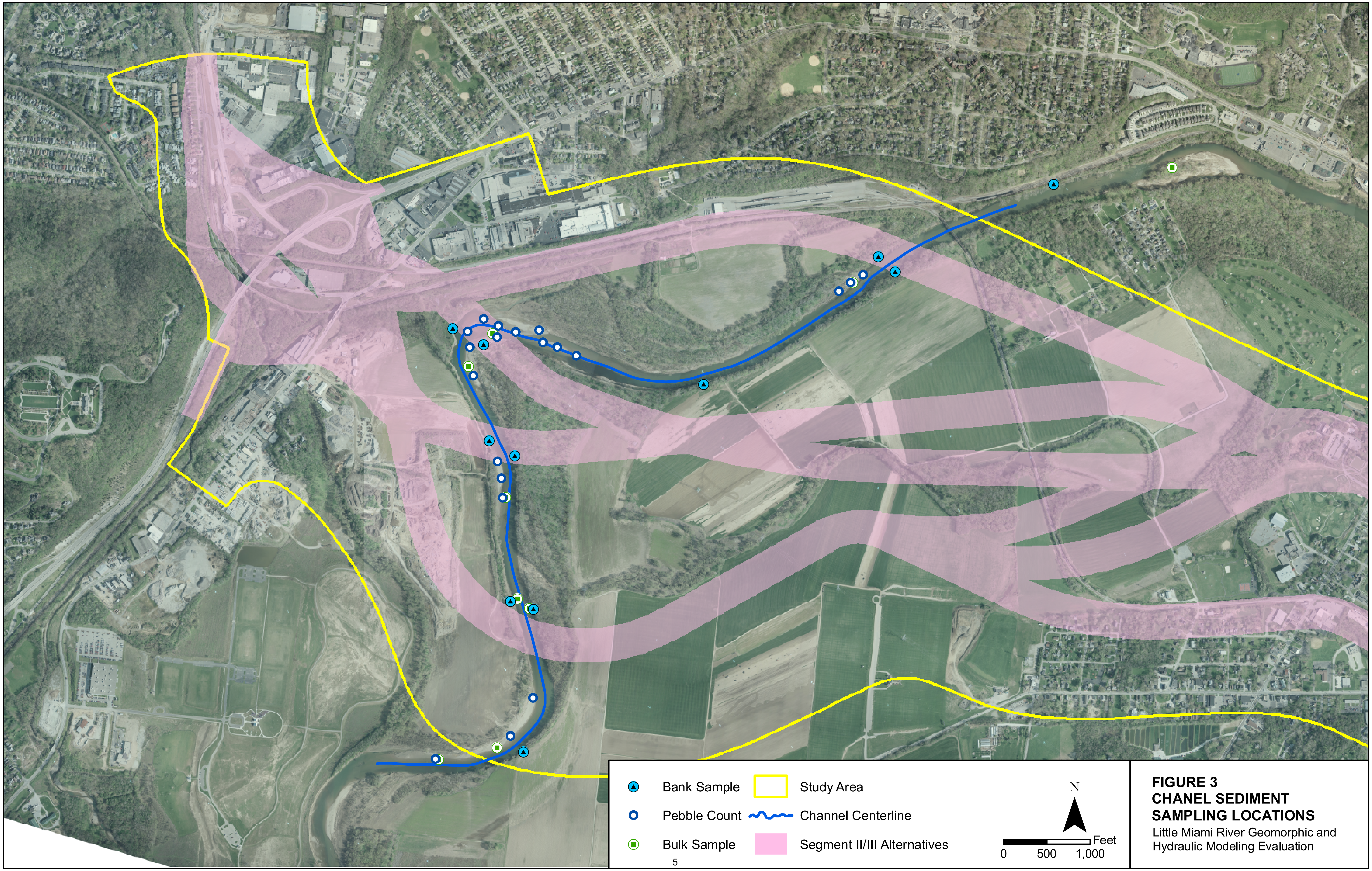

\\SFO31029951\PROJECTS\LITTLEMIAMIRIVER\GIS\MAPFILES\CHANELSEDIMENTSAMPLINGLOCATIONS.MXD FIG3_CHANELSEDIMANTSAMPLINGLOCATIONS.PDF AFALZONE 1/24/2009 22:12:11

Miami River and the East Fork Little Miami River (Figure 1). The Little Miami River is the dominant watershed with an area of 1,203 square miles at USGS Gage 03245500 "Little Miami River at Milford OH" (Koltun 2003), which is located 1.5 miles upstream of the confluence with the East Fork Little Miami River. The East Fork Little Miami River drains a watershed area of 476 square miles at USGS Gage 03247500 "East Fork Little Miami River at Perintown OH" (Koltun 2003), which is located 6.3 miles upstream of the confluence with the Little Miami River. Figure 4 shows the locations of the USGS streamflow gage stations used in this analysis. An additional 79 square miles downstream of the USGS gages drain to the Little Miami River in the Study Area through the East Fork (24 square miles) and the mainstem (55 square miles), giving the Study Area a total watershed area of 1,758 square miles.

The hydrology of the Little Miami River in the Study Area has been altered by flow regulation at two upstream reservoirs. Flow is regulated on the Little Miami River at Caesar Creek Lake and on the East Fork Little Miami River at William H. Harsha Lake (East Fork Lake) (Figure 1). Both reservoirs are operated by the U.S. Army Corps of Engineers (USACE) and both became operational in 1978 (USACE 2008a). Caesar Creek Lake has a contributing watershed area of 237 square miles and a storage capacity of 242,209 acre feet (USACE 2008b). William H. Harsha Lake has a contributing watershed area of 342 square miles (USACE 2008a) and storage capacity of 284,468 acre feet (USACE 2008b). Together, these two reservoirs regulate flows from nearly 33 percent of the watershed that drains to the Study Area.

Several manipulations and analyses of available hydrology data were required to accurately describe the hydrologic conditions in the Study Area and to assess the impacts of flow regulation from reservoir operations. First, daily average discharge data from the two upstream USGS gages were combined to produce a historical daily average discharge record for the Study Area. Next, annual instantaneous peak discharges for the two upstream USGS gages were combined to produce an annual peak discharge record for the Study Area. A flood frequency analysis was then conducted using this peak discharge record. Finally, a flow concurrence analysis was completed to determine the proportion of Little Miami River floods that are controlled by backwater conditions on the Ohio River downstream.

3.1 Daily Average Discharge Combination

Daily average discharge data from the two most downstream gages on the Little Miami River (USGS Gage 03245500 Little Miami River at Milford OH) and the East Fork Little Miami River (USGS Gage 03247500 East Fork Little Miami River at Perintown OH) (Figure 4) were combined to create a composite stream discharge record for the Study Area. Daily average discharge data was available for both gages for a period of record from 1926 to 2008.

The combined daily average discharge in the Study Area is plotted in Figure 5. The effect of dam construction can be seen in the significant reduction in maximum daily average discharge after 1975. The maximum daily average discharge was nearly 90,000 cfs prior to 1975, with many peaks greater than 50,000 cfs. Maximum daily average discharges have all been lower than 50,000 cfs since 1975, and most have been lower than 40,000 cfs. Most of the maximum daily average discharges on the Little Miami River occur in late fall, winter, and

FIGURE 4
USGS GAGE LOCATION MAP
Little Miami River Geomorphic and Hydraulic Modeling Evaluation

spring throughout the period of record. In contrast to the changes in maximum daily average discharge associated with reservoir regulation, the mean daily average discharge has increased nineteen percent from approximately 1,708 cfs prior to 1975 to approximately 2,030 cfs after 1975. Because both extreme and average hydrologic conditions have changed with the operation of the upstream reservoirs it is important to consider ongoing and future reservoir operations in any evaluation of future channel stability. Base flows in the Study Area are relatively variable throughout the period of record, reaching minimum values of slightly less than 100 cfs with some regularity. These low flows do not directly contribute to changes in channel morphology; however, they may contribute indirectly through their influence on the extent of riparian vegetation along channel margins.

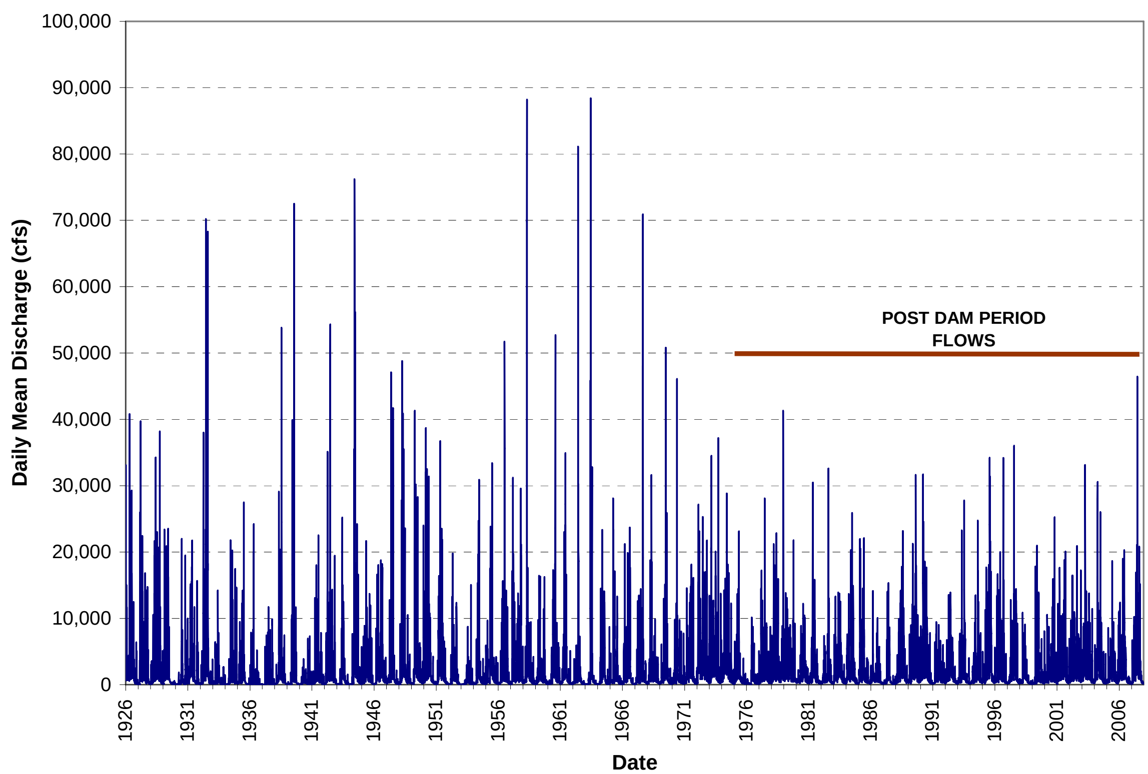

Figure 5: Combined daily average discharge for USGS Gage 03245500 Little Miami River at Milford OH and USGS Gage 03247500 East Fork Little Miami River at Perintown OH.

3.2 Annual Peak Discharge Analysis

Annual peak discharges in the Study Area were estimated by combining the instantaneous peak discharge records from the two upstream gages. Annual peak discharges occurred on the same day at these two gages 51 percent of the time during the 82 year period of record, and within one day of each other 57 percent of the period of record. Peak discharges from the two upstream gages were added together for these two conditions. For the 43 percent of peak discharges that occurred more than one day apart, the following approach was used to estimate a combined peak discharge. First, the instantaneous peak discharge on the East Fork on the same day as the peak discharge on the Little Miami River was determined from hourly discharge data available for the period 1990 to 2006 and added to the instantaneous peak discharge on the Little Miami River. This accounted for 14 percent of the 43 percent of peaks that occurred more than one day apart.

Next, a linear regression analysis was conducted to develop a relationship between annual peak discharge and daily average discharge at gage 03247500 on the East Fork using the period of record data from that gage (Figure 6) between 1926 and 1990. Peak discharge values for the East Fork were then calculated using the regression equation for each year when the peak discharge on the East Fork occurred more than one day before or after the peak discharge on the Little Miami River. These calculated peak discharges accounted for the remaining 29 percent of the 43 percent of peaks that occurred more than one day apart. Finally, these calculated peak discharges for the East Fork were added to the Little Miami River peak discharges to complete the annual instantaneous peak discharge data set for the Study Area.

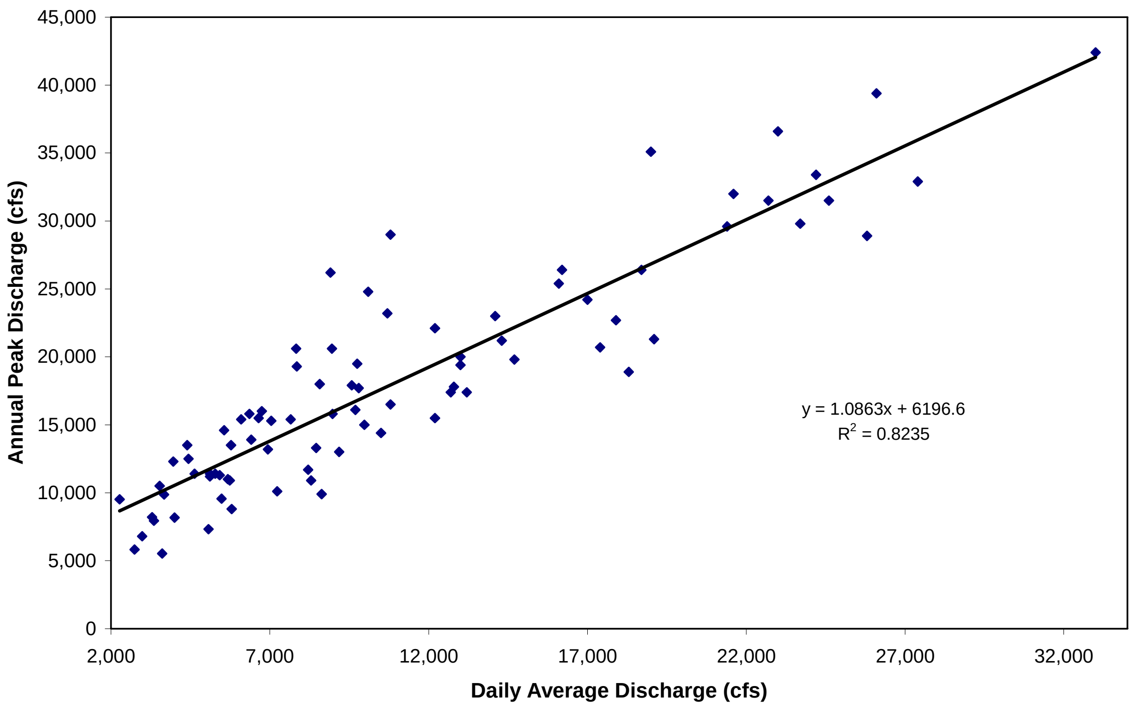

Figure 6: Linear regression for daily average and annual peak discharge at USGS Gage 03247500 East Fork Little Miami River at Perintown OH.

The combined annual peak discharge record for the Study Area is plotted in Figure 7. This analysis also shows how reservoir operation has significantly reduced instantaneous peak discharges in the Little Miami River since 1975. Instantaneous peak discharge has been reduced from over 110,000 cfs prior to 1975 to less than 80,000 cfs after 1975. Prior to 1975, instantaneous peak discharges during dry years were typically greater than 20,000 cfs. After 1975, dry year peak discharges have decreased to 10,000 cfs or less. Some of this change could be attributed to a drier climate since 1975, however most is likely due to reservoir regulation of downstream discharge. River dynamics such as lateral migration typically respond to this type of flow regime modification, so the flood frequency analysis and subsequent hydraulic modeling described in the following sections has been conducted using hydrology reflecting the entire period of record and the post-1975 period of record. In general, river processes such as erosion, deposition, and vegetation succession are slowed with this kind of hydrologic change. Therefore, estimates of long-term historical channel change may over-predict future rates of change.

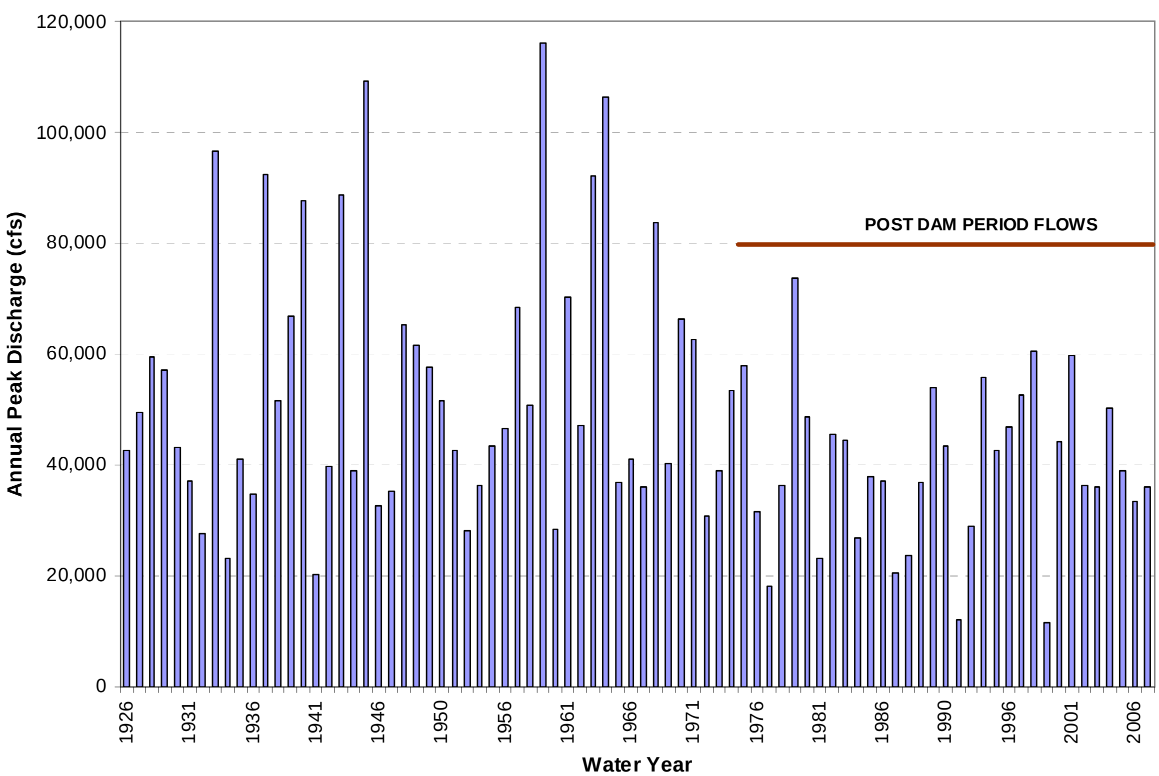

Figure 7: Combined annual peak discharge in the Study Area developed from USGS Gage 03245500 Little Miami River at Milford OH and USGS Gage 03247500 East Fork Little Miami River at Perintown OH.

3.3 Log Pearson Type III Distribution Flood Frequency Analysis

A flood frequency analysis of the combined annual peak discharge of the Little Miami River and the East Fork Little Miami River was conducted to predict the peak discharge for a given recurrence interval in the Study Area. The Log Pearson Type III Distribution approach is a statistical technique used to construct a frequency distribution of discharges in a river. The advantage of this technique is that the log-normally distributed discharge values can be extrapolated for flood events whose recurrence interval is beyond the observed flood events. A flood recurrence interval is defined as the time period during which a flood event of a given magnitude is expected to recur. To account for the impact of reservoir operations on the Little Miami River in the Study Area, flood frequencies were calculated using discharges during the period before dams were constructed (1926-1975), the post-dam construction period (1976-2007), and the full period of record (1926-2007). Construction of both dams in the Little Miami River watershed was completed by 1978, however, the reservoirs most likely began filling between 1975 and 1976. Therefore, 1975 was used as the delineation point for the impact of dam construction and reservoir operation.

The results of the Log Pearson Type III flood frequency analysis quantify the changes in hydrology caused by dam construction and reservoir operation (Table 1 and Figure 8). Table 1 summarizes flood magnitudes for the complete period of record (1926-2007), the pre-dam period (1926-1975), and the post-dam period (1976-2007) for recurrence intervals of 1, 2, 5, 10, 25, 50, 100, and 200 years. The 2-year discharge, often considered to be a channel forming discharge, has been reduced by nearly 10,000 cfs (22 percent) in the post-1975 period. This change could have important ramifications on channel evolution. The 100-year discharge has also been reduced by 67,000 cfs (49 percent) from the pre-dam to post-dam period. Because of the magnitude of the hydrologic changes associated with the operation of the upstream dams and reservoirs, future dam and reservoir operations should be considered in the prioritization and eventual design of bridge crossing locations in the Study Area.

TABLE 1
Flood frequency analysis results for the Little Miami River for the period of record 1926 to 2007

Flood Flow Return Period (Years)	Pre-1975 Flood Discharge (cfs)	Complete Data Set Flood Discharge (cfs)	Post-1975 Flood Discharge (cfs)
1	19,684	13,615	9,522
2	49,913	45,507	39,017
5	71,194	64,909	52,059
10	86,078	76,878	58,217
25	105,689	91,013	63,934
50	120,851	100,849	67,073
100	136,530	110,100	69,519
200	152,773	118,962	71,436

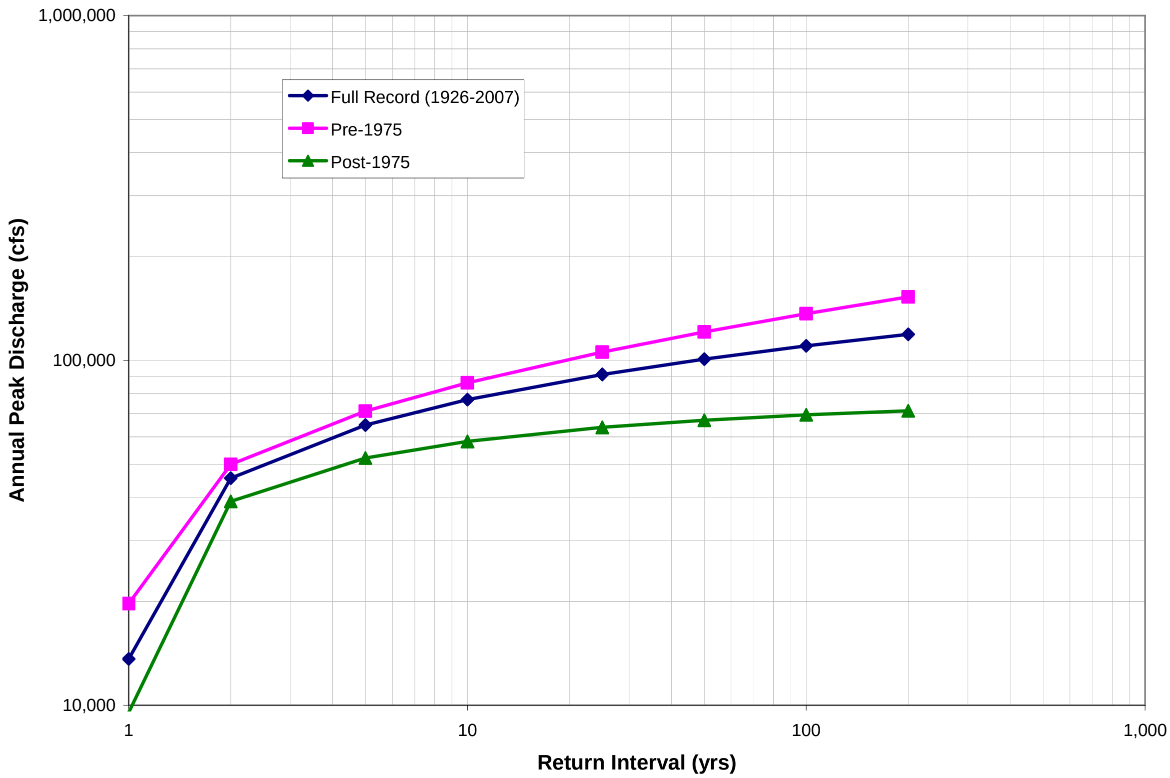

Figure 8: Combined annual peak discharge for the Study Area developed from USGS Gage 03245500 Little Miami River at Milford OH and USGS Gage 03247500 East Fork Little Miami River at Perintown OH.

3.4 Flow Concurrence Analysis

Representatives of both the Motes and Turpin farms (Motes and Turpin personal communications 9/8/08) have noted that "downvalley floods" (i.e. Little Miami River peak discharges not controlled by backwater influence of simultaneous peak discharge in the Ohio River) cause the greatest channel change on the Little Miami River, and that "backwater floods" (i.e. Little Miami River peak discharges controlled by Ohio River backwater influence) do not cause significant channel change. A peak discharge concurrence analysis was conducted to estimate the likelihood of simultaneous peak discharges on the Little Miami River and the Ohio River downstream, and to characterize the general magnitude and frequency of downvalley floods.

Using historical stage data from USGS gage #03255000 on the Ohio River (Figure 4) and the peak discharge record for the Study Area, a downvalley flood was assumed to occur if the water surface elevation on the Ohio River was less than or equal to the elevation midway between the channel invert and top of bank (approximately 464.5 feet msl) at the downstream end of the Study Area on the Little Miami River on the day of the annual peak discharge on the Little Miami River. This evaluation was only possible for the period between 1988 and 2007, when stage data was available from the Ohio River gage.

Approximately 39 percent of the Little Miami River peak discharges were determined to be downvalley floods based on this analysis. Of this 39 percent, approximately 71 percent of the Little Miami River peak discharges were less than the post-1975 2-year discharge of 39,017 cfs. Most of the Little Miami River peak discharges with return intervals greater than two years during this period were associated with high peak stage on the Ohio River and were therefore backwater floods. It is likely that most other large Little Miami River peak discharges in the period of record were also backwater floods. Therefore, assuming these flood characteristics are representative of future peak discharge conditions, it is the relatively frequent peak flows on the Little Miami River that are most important with respect to channel stability. These flows are the focus of the hydraulic modeling analyses described later in this report.

4 Historical Channel Morphology Analysis

Systematic analyses of historical aerial photographs of river corridors can be used to assess and quantify long-term changes and trends in channel morphology. Lowland alluvial channels typically meander across their floodplains over long time scales, creating complex landforms and habitat while adjusting channel planform, geometry, and profile. The Little Miami River is a sinuous lowland alluvial river with active meander bends that have migrated across the floodplain in the Study Area. However, channel change and lateral migration on the Little Miami River is much more extensive in some reaches than in others. The objective of this analysis was to assist in the selection of the most sustainable reaches for a clear span crossing of the Little Miami River by quantifying long-term, systematic channel change and lateral migration through time.

Historical aerial photographs were obtained in digital format for 18 individual years between 1932 and 2005 (Table 2). The 1948, 1964, 1981, and 1986 aerial photographs were rectified using ArcGIS software (Environmental Systems Research Institute, 2007) and integrated into the Project GIS. The 1932, 1938, 1950, 1956, 1962, 1968, 1975, 1977, and 1990 digital images were obtained in rectified format and the 1994, 2000, 2004, and 2005 digital images were obtained in orthorectified format from the USGS. Orthorectified images correct for distortion caused by the roll, pitch, and yaw of the aircraft when the image was taken and result in more accurate images than rectified images, which are stretched to fit a set of control points. The 2007 aerial photograph was used as the base map for rectification of the historical photographs. The root mean square (RMS) error for most of the rectified photos was less than 10 feet; however a few images had RMS error of nearly 50 feet. Photos from ODOT had no error quantification. Measurements of channel change from photos with higher RMS error have more uncertainty than measurements from photos with lower RMS error. Table 2 summarizes the aerial photo data, including the RMS error where available.

Based on observed historical channel changes and general geomorphic characteristics from this evaluation, past studies, and other data collection efforts on the river or in the watershed, the Little Miami River was first delineated into geomorphic reaches in the Study Area. The top of the channel bank along both sides of the channel was then digitized on each historical aerial photograph to illustrate and allow quantification of channel migration.

Next, channel migration was measured as the distance between two top of bank lines representing the same bank (i.e. right or left) in different years. The quantification of channel migration rates is described in more detail in section 4.2 below.

TABLE 2
Historical aerial photography for the Little Miami River Study Area

Flight Date	Source	Daily Average Discharge (cfs)	Scale	Resolution	Average RMS Error Range (feet)
4/10/2007	ODOT	866	Not Available	0.5 ft	Not Available
6/22/2005	NAIP	317	Not Available	2 m	Not Available
6/24/2004	NAIP	661	Not Available	1 m	Not Available
10/20/2000	NAPP	654	Not Available	1 m	Not Available
4/1/1994	OGRIP	1,106	Not Available	1 m	Not Available
1990	ODOT	Not Available	Not Available	5 ft	Not Available
3/24/1986	ODOT	1,464	1:6,000	Not Available	2.8 – 25.9
April 1981	ODOT	Not Available	1:12,000	Not Available	5.0 - 49.3
1977	ODOT	Not Available	Not Available	5 ft	Not Available
1975	ODOT	Not Available	Not Available	5 ft	Not Available
1968	ODOT	Not Available	Not Available	5 ft	Not Available
December 1964	ODOT	Not Available	1:12,000	Not Available	8.7 - 46.7
1962	ODOT	Not Available	Not Available	5 ft	Not Available
1956	ODOT	Not Available	Not Available	5 ft	Not Available
1950	ODOT	Not Available	Not Available	5 ft	Not Available
May 1948	ODOT	Not Available	1:24,000	Not Available	16.9 - 43.8
1938	ODOT	Not Available	Not Available	5 ft	Not Available
1932	ODOT	Not Available	Not Available	5 ft	Not Available

Notes: Daily discharge is a combination of flow data from USGS Gage 03245500 Little Miami River at Milford OH and USGS Gage 03247500 East Fork Little Miami River at Perintown OH, as described in the hydrology section of this report.

There are two primary geomorphic reach types in the Study Area: active meander bend reaches and stable straight reaches (Figure 9). In some locations the natural dynamics of portions of a reach have been altered by bank armoring or other human interventions. However, in general, the historical rates of channel change are significantly higher in the active meander bends than they are in the stable straight reaches. Geomorphic reaches 1, 2, and 3 are upstream of the Study Area and illustrate characteristics of nearby historical

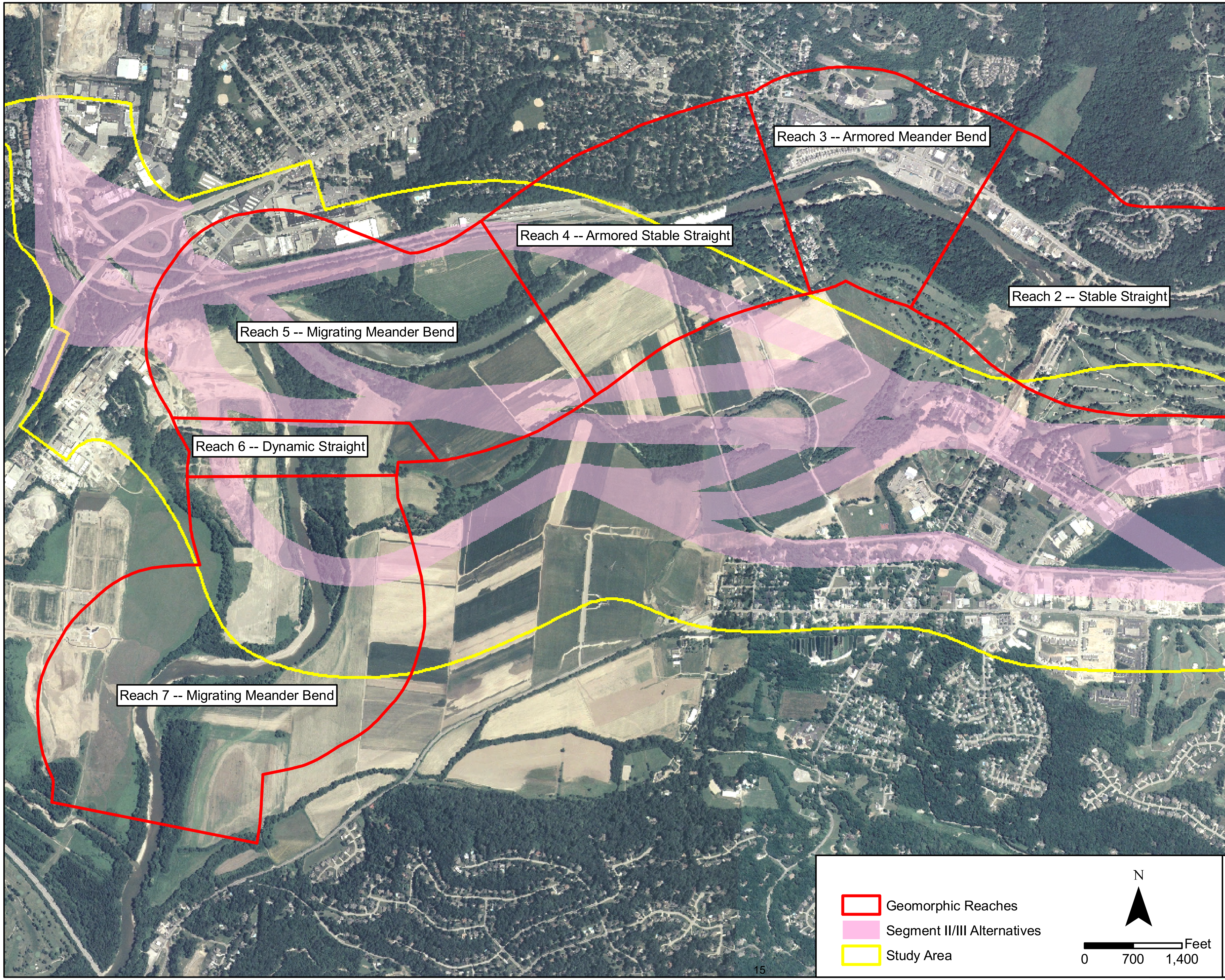

FIGURE 9
GEOMORPHIC REACHES

Little Miami River Geomorphic and Hydraulic Modeling Evaluation

\\SFO31029951\PROJECTS\LITTLEMIAMIRIVER\GIS\MAPFILES\GEOMORPHICREACHESV2.MXD GEOMORPHICREACHESV2.MXD AFALZONE 1/25/2009 22:10:28

channel evolution in a way that provides useful context for interpreting changes in the Study Area. Geomorphic reaches 4, 5, 6, and 7 are either partly or completely within the Study Area. The following sections summarize general historical geomorphic conditions in each geomorphic reach and present historical average annual lateral migration rates.

4.1 Geomorphic Reach Narrative Descriptions

As the Little Miami River nears its confluence with the Ohio River, it flows across a broad alluvial valley. In the Study Area, the channel has migrated across the valley floor and is presently confined along the northern valley wall. The Conrail railroad tracks are located at the toe of the hills that form the northern valley wall and act as a barrier to channel migration in some locations. The channel is further confined by riprap and other armoring that has been installed on channel banks to reduce bank erosion adjacent to sensitive infrastructure. In general, the north bank is confined by topography or infrastructure and armoring, while the south bank is less confined by primarily agricultural land uses adjacent to the channel. As is typical in lowland alluvial rivers, the meander bends in the Study Area are migrating downstream and laterally in the direction of the outside of their bends. The amount of channel migration observed in the historical aerial photographs shows that the Little Miami River is geomorphically active and prone to future channel migration in the Study Area, especially in certain reaches.

4.1.1 Reach 1: Migrating Meander Bend

This reach is upstream of the Study Area and is characterized by a meander bend migrating laterally toward the left bank (Figure 9). A point bar is clearly visible on the inside of this meander bend in 2005. The rate of change to this point bar accelerated after 1975, which is a typical response to flow regime alteration from reservoir regulation. A second large bar is present on the outside of this meander, possibly from material eroded from the upstream bank. Between 1932 and 1956, a mid-channel bar was present just downstream of the meander bend. This downstream bar may have deflected the thalweg towards the opposite bank, which shows signs of past erosion. The mid-channel bar most likely washed out during the January 22, 1959 flood, which had a peak discharge of 116,100 cfs. However, the channel does not appear to have been affected by the March 10, 1964 peak discharge of 106,300 cfs. To arrest bank erosion along the outside bend in this reach, riprap was recently placed at the apex of the bend. This could accelerate future erosion of the opposite bank downstream of the meander. Floodplain land use in this reach has remained relatively consistent on the north bank of the channel, while development has increased on the south bank. Homes surrounded by agricultural fields are present in 1932 just downstream of the apex of the bend. These homes and fields were replaced in the late 1990s with a sports complex and related facilities. The long-term dynamics observed in this migrating meander bend reach are consistent with conditions observed in migrating reaches in the Study Area and highlight the need for caution when considering a bridge crossing in an actively meandering reach.

4.1.2 Reach 2: Stable Straight

This reach is upstream of the Study Area (Figure 9) and is characterized by a stable, shallow bend with a mid-channel island or bar downstream of the Church Street Bridge. At low flows, this island or bar is continuous with the right bank of the channel. The bar or island is a consistent feature in the channel between 1932 and 2005, although the size and shape changes during this period. The channel shows no significant change or migration after peak discharges have passed through this reach. The north bank floodplain has increasingly become encroached by development between 1932 and 2005. The south bank has remained vegetated with mature riparian vegetation downstream of the Church Street Bridge. Upstream of the bridge, a golf course began to encroach the riparian zone in the late 1970s. Based on the historical stability of this reach, it is unlikely that the reach will experience significant channel migration in the future. The relatively stable nature of this straight reach is consistent with conditions in straight reaches in the Study Area, illustrating the higher suitability of straight reaches for sustainable clear span channel crossings.

4.1.3 Reach 3: Armored Meander Bend

This reach is also upstream of the Study Area (Figure 9). Historically, the railroad ran adjacent to the north bank of this geomorphic reach. Urban development began in the 1980s and has replaced the railroad on the right bank in the upstream portion of this reach. There is a large bar on the left bank towards the downstream end of the reach with a secondary channel that cuts across the back of the bar that appears to be increasing in size through time (especially since 1975). The secondary channel remains relatively clear of vegetation through time, suggesting that high flows regularly enter and scour this channel. The progradation of this bar, combined with urban development along the right bank, have forced a sharp bend in the channel, and this bend appears to have been armored to protect against local channel erosion. This armoring could limit future migration of this meander bend; however, it could also induce erosion of a nearby bank in this reach or in the next geomorphic reach downstream. Because the next downstream reach is within the Study Area, alternatives to the armoring in this reach should be considered. In addition, because the dynamic nature of this reach could translate downstream in the future, clear span crossings in the downstream geomorphic reach should be located away from the upstream reach boundary.

4.1.4 Reach 4: Armored Stable Straight

This geomorphic reach is mostly within the Study Area (Figure 9). The north bank of this reach is paralleled by and crosses under the railroad. Upstream of the bridge crossing, lateral channel migration towards the north bank is controlled by the railroad at the toe of a bluff. Downstream of the bridge on the north bank, a secondary channel exits the primary channel and appears to be inundated only during high flows. Sediment deposition appears to have periodically filled this channel, which rejoins the Little Miami River near the boundary of the next geomorphic reach downstream. Sediment deposition is readily apparent in the secondary channel in 1968 and 1977, but has been removed by 1981, either by high flow scour or manual excavation. Flows in this geomorphic reach may be directed towards the secondary channel by the bridge piers supporting the railroad bridge. However, the scour and deposition observed in the aerial photographs does not seem to be correlated with peak discharges on the Little Miami River, so the condition of the secondary channel may be more strongly influenced by human management activities. On the south bank, across from the secondary channel, agricultural fields extend to the channel bank and do not appear to induce lateral channel migration. At the downstream end of this reach, the north bank regularly experiences erosion and scour in the vicinity of the secondary channel as it transitions into the next downstream geomorphic reach, one that is characterized by relatively high channel instability. Historically, the majority of this reach has experienced little channel migration and is likely to remain stable in the future. However, the middle portion of this geomorphic reach appears to be more stable than the upstream and downstream portions of the reach.

4.1.5 Reach 5: Migrating Meander Bend

This geomorphic reach encompasses the "Horseshoe Bend" (Figure 9), and has experienced the most channel migration in the Study Area. There was an abandoned channel downstream of the current channel in 1932, and by 1938 this abandoned channel and oxbow lake had been filled for agriculture. Agricultural uses were slowly converted to riparian forest on both the north and south sides of the channel between 1932 and 1981. As the channel has migrated downstream and towards the outside of the right bank meander bend, an expansive point bar has formed on the inside of the bend. Two peak discharges on April 20, 1940 (87,800 cfs) and May 6, 1945 (109,300 cfs) significantly altered the channel planform in this geomorphic reach. Before 1940, the channel had a gentle bend with a well developed point bar. The 1940 and 1945 peak discharges deposited sediment and debris on the point bar, forcing the channel to migrate laterally. By 1956, the former channel path had become fully vegetated.

Significant erosion and deposition has also occurred upstream of the Horseshoe Bend where a small tributary channel enters the Little Miami River. This tributary is connected to the secondary channel that exits the Little Miami River in the upstream geomorphic reach. The lateral extent of this secondary channel appears to coincide with the margin of the Little Miami River from the 1930s. It appears that as the Little Miami River has migrated downstream and eroded the outside of its meander bend between 1975 and 1994 this area has been reclaimed by riparian vegetation. However, a secondary channel still remains and likely carries some flow during peak discharges. Given the extremely dynamic nature of this geomorphic reach, it has low suitability for a clear span bridge crossing.

4.1.6 Reach 6: Dynamic Straight

This short geomorphic reach is located between two very active geomorphic reaches in the Study Area (Figure 9), yet it has remained relatively stable since 1938. This geomorphic reach did not appear to be significantly influenced by peak discharges between 1932 and 2005, despite the fact that peak discharges caused significant channel migration in the upstream and downstream geomorphic reaches. However, if Horseshoe Bend continues to migrate downstream and laterally, the channel could eventually cut off the meander and form an oxbow lake and realigned channel that could extend into this geomorphic reach. If a channel cutoff were to occur, this geomorphic reach would likely be significantly altered. A landfill operation was started in this reach in the early 1990s and continues at least through 2005. The landfill operation is buffered from the channel by agricultural fields, but may still influence channel dynamics during high discharge periods.

This geomorphic reach is more suitable for a clear span crossing than the upstream reach; however its overall suitability is still low because of the potential for major channel change induced by a future meander bend cutoff upstream. The extremely narrow radius of curvature of Horseshoe Bend indicates that a cutoff is likely to occur during the design life of the proposed river crossing. Such a cutoff would shorten the channel length in this portion of the study area, effectively increasing the local channel slope, flow velocities, and erosive energy. This change could result in even higher short term lateral channel migration rates than those observed in Horseshoe Bend, as Horseshoe Bend has been armored while armoring would not be feasible on the newly created meander bend. Further, anticipating the uncertain location and dimensions of a cutoff in the design of a clear span crossing would be extremely difficult.

4.1.7 Reach 7: Migrating Meander Bend

This is the downstream-most geomorphic reach in the Study Area (Figure 9) and it is characterized by two migrating meander bends. Between 1932 and 2005, the meander bends have become tighter and have migrated downstream. Mid-channel bars were scoured from the channel after the May 6, 1945 peak discharge of 109,300 cfs. After the January 22, 1959 peak discharge of 116,100 cfs, the channel migrated about 200 feet at the upstream meander bend in the reach. Migration of the outside of this meander bend continues along with growth of the point bar on the inside bend. The September 14, 1979 peak discharge of 73,800 cfs caused significant scour of the point bar on the inside of the downstream meander bend. Despite similar change that occurred during the peak discharge on April 16, 1998, the upstream meander bend has been relatively stable since 1975, especially compared to the downstream meander bend, which has continued to migrate.

A small tributary enters the Little Miami River in this geomorphic reach on the left bank near the upstream end of the reach. The Little Miami River is connected to this tributary by a secondary channel with a small island or mid-channel bar along the channel margin. In 1932, an abandoned channel was located approximately 1,500 feet from the left bank of the Little Miami River. The island or mid-channel bar has clearly migrated downstream of its location in 1932, particularly between the 1930s and the early 1960s. This movement appears to have slowed considerably or ceased since 1960, possibly because peak flows of the post-reservoir regulation era no longer have sufficient energy to mobilize the island or mid-channel bar deposits. Although lateral channel migration continues to occur in this geomorphic reach, the rate of channel migration has slowed significantly over the past several decades. Still, given the dynamic nature of this reach and the channel complexity associated with the meander bends and tributary connection, it has only moderate suitability for a clear span crossing.

4.2 Quantification of Historical Channel Change in Geomorphic Reaches

Short-term maximum and long-term average annual channel migration rates were calculated for the right bank and left bank (looking downstream) in the four geomorphic reaches in the Study Area to quantify lateral channel migration. The short-term maximum rate of channel migration was calculated by dividing the distance between top of bank lines by the number of years in the period of maximum channel migration. Long-term average annual rate of channel migration was calculated by dividing the distance of channel migration on each bank (the maximum extent of the top of bank lines) by the seventy-five year period covered by available aerial photography. Both the short-term maximum and long-term average annual lateral migration rates were calculated at the locations of minimum and maximum long term average annual migration within each geomorphic reach, and at proposed bridge crossing locations in each geomorphic reach. Figure 10 and Table 3 summarize the results of this analysis. The lateral migration rates reinforce the narrative descriptions of change in each geomorphic reach and can be used to further assess reaches for potential clear span bridge crossings, and to specify crossing design requirements that ensure the crossing will not influence the Little Miami River over the life of the bridge.

Geomorphic reach 5 has the highest average annual lateral migration rate (16.8 ft/yr) in the Horseshoe Bend and is likely to continue to migrate rapidly in the future. The short-term maximum bank migration rate in geomorphic reach 5 was the second highest in the Study Area (100.5 ft/year). Geomorphic reach 7, at the downstream end of the Study Area, has the second highest long-term average annual migration rates (10.6 ft/yr) and the highest short-term annual bank migration rate (122.6 ft/yr). Geomorphic reach 6 has the second lowest long-term average annual migration rate (8.5 ft/yr), but could be significantly altered if the Horseshoe Bend meander were to cut-off. The short-term maximum migration rate in geomorphic reach 6 (54 ft/yr) is moderate, which suggests that migration in this reach is consistent over time in this straight reach. The long-term migration rates throughout geomorphic reach 4 are consistently lower than migration rates in the other geomorphic reaches (0.7 ft/yr to 3.0 ft/yr). For the most part, the short-term maximum migration rates are also low in this geomorphic reach (10.5 ft/yr to 32.4 ft/yr), except for the right bank at cross section 3 (94.8 ft/yr), which is just downstream of the head of the back channel that extends downstream to Horseshoe Bend. This back channel was digitized as the top of bank in four different years, suggesting a pattern of scour and deposition. The top of bank line switched locations between the 2005 and 2007 aerial images, which resulted in an artificially high annual average rate due to the short, two year period between the images. The combination of a low long-term and high short-term migration rate suggests that the channel has remained relatively stationary over time, and experienced the majority of channel migration over a short period.

5 Two Dimensional Hydraulic and Sediment Transport Modeling

This section describes the hydraulic modeling analysis conducted to assist in evaluating the suitability of the geomorphic reaches in the Study Area for potential clear span bridge crossings. The goal of this effort was to predict and analyze site-specific hydraulics in the Study Area to help determine which geomorphic reaches are likely to be the most stable, and therefore the most suitable, for a clear span bridge. This task builds on the historical and current understanding of hydrology and hydraulics in the Study Area to provide a predictive capability with respect to future channel morphology and stability. The following sections describe the modeling software used in the analysis, the setup and application of the two-dimensional hydraulic and sediment transport models, the use of the Hydraulic Engineering Center's River Analysis System (HEC-RAS) model in developing and refining

TABLE 3

Summary of average annual channel migration rates

Geomorphic Reach	Measurement Location	Channel Bank (looking downstream)	1932-2007 Migration Distance (ft)	1932 – 2007 Avg. Annual Migration Rate (ft/yr)	Short Term Maximum Migration Distance (ft)	Short Term Maximum Migration Period (years)	Short Term Maximum Migration Rate (ft/yr)
Reach 4 -- Armored Stable Straight Reach	Minimum (XS1)	Right	60	0.8	42	1975 - 1977	21.2
		Left	50	0.7	21	2005 - 2007	10.5
	Bridge (XS2)	Right	107	1.4	96	1990 - 1994	24.1
		Left	109	1.4	65	1975 - 1977	32.4
	Maximum (XS3)	Right	222	3.0	190	2005 - 2007	94.8
		Left	143	1.9	49	1975 - 1977	24.6
Reach 5 -- Migrating Meander Bend	Minimum (XS4)	Right	207	2.8	186	2005 - 2007	92.9
		Left	111	1.5	33	2004 - 2005	33.1
	Maximum & Bridge (XS5)	Right	1259	16.8	402	1990 - 1994	100.5
		Left	1031	13.8	107	2005 - 2007	53.4
	Bridge 2 (XS6)	Right	241	3.2	97	1962 - 1964	48.2
		Left	402	5.4	258	1932 - 1938	43.0
Reach 6 -- Dynamic Straight Reach	Minimum (XS7)	Right	247	3.3	86	1962 - 1964	43.2
		Left	516	6.9	372	1932 - 1938	61.9
	Maximum (XS8)	Right	435	5.8	243	1932 - 1938	40.5
		Left	640	8.5	324	1932 - 1938	54.0
Reach 7 -- Migrating Meander Bend	Minimum (XS9)	Right	196	2.6	61	1962 - 1964	30.7
		Left	83	1.1	81	1948 - 1950	40.6
	Bridge (XS10)	Right	292	3.9	76	1962 - 1964	38.1
		Left	301	4.0	142	1948 - 1950	70.8
	Maximum (XS11)	Right	796	10.6	245	1962 - 1964	122.6
		Left	758	10.1	109	1948 - 1950	54.2

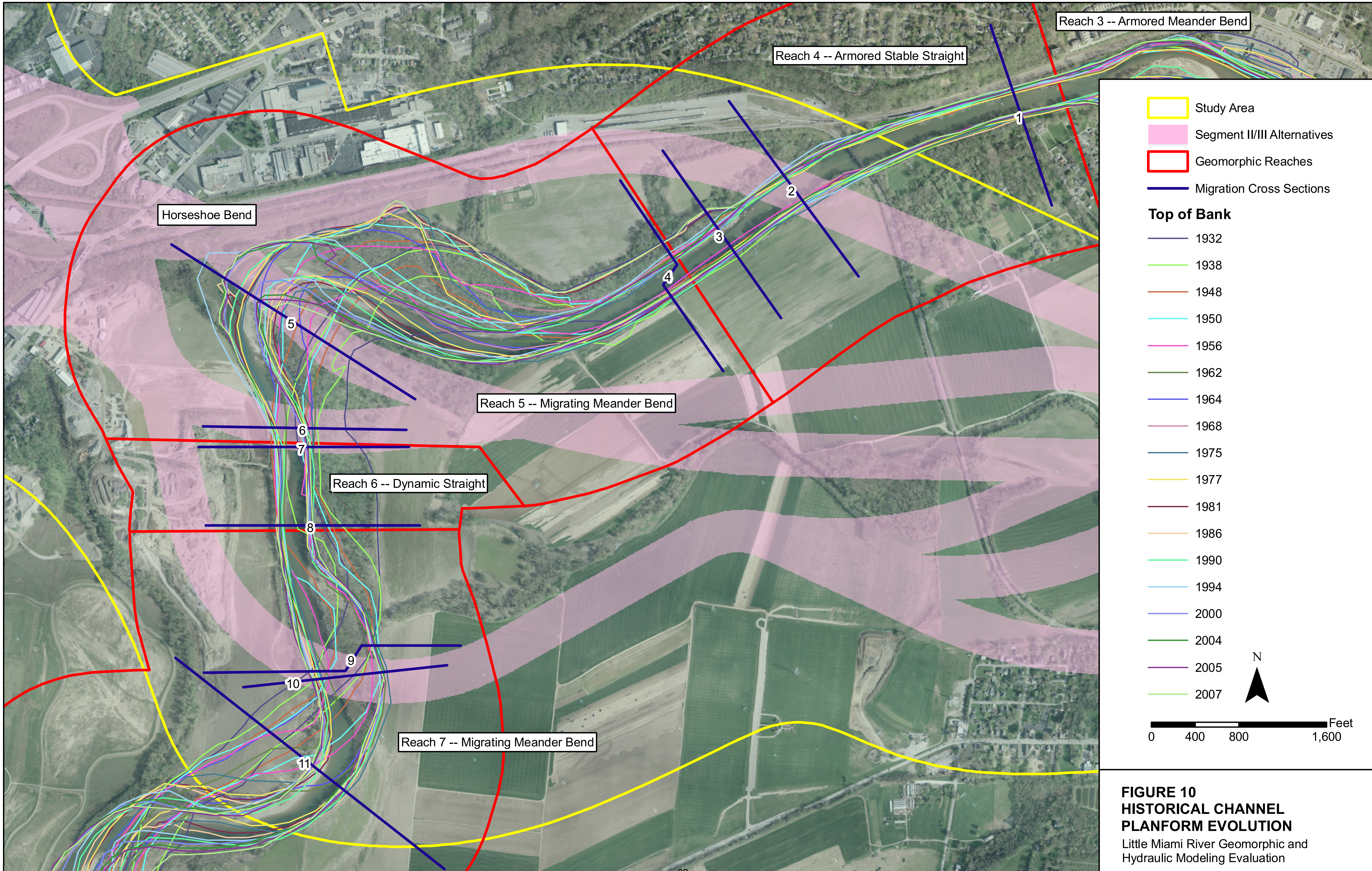

FIGURE 10
HISTORICAL CHANNEL PLANFORM EVOLUTION
Little Miami River Geomorphic and Hydraulic Modeling Evaluation

\\SFO31029951\PROJECTS\LITTLEMIAMIRIVER\GIS\MAPFILES\TOBFIGUREV2.MXD TOBFIGUREV2.MXD AFALZONE 1/29/2009 06:15:35

bathymetric and topographic information for use in the multi-dimensional model, and the interpretation of numerical model results with respect to the project goals.

5.1 Modeling Approach

The Surfacewater Modeling System (SMS) is a collection of multi-dimensional hydrodynamic, constituent transport, and sediment transport models packaged with pre- and post-processing tools. The SMS software is distributed and supported by Environmental Modeling Systems, Inc. (now Aquaveo), and is built on the USACE TABS Modeling System. The software package contains the RMA-2 hydrodynamic model, the RMA-4 constituent transport model, and the SED2D sediment transport model, among others. The HEC-RAS hydraulic model was also used in this analysis. HEC-RAS, developed by the USACE, is a one-dimensional model that is used widely in river and floodplain modeling studies. HEC-RAS provides cross-section averaged results, and thus cannot account for lateral variations in velocities in a complex river channel or floodplain.

5.2 Model Setup

A two dimensional model grid was constructed for a 2.4 mile reach of the Little Miami River extending from the railroad bridge downstream to a location near Otto Armleder Memorial Park (Figure 11). Model topography was derived from a combination of LIDAR data and a field survey of channel cross sections and a longitudinal thalweg profile completed by Stantec. The available LIDAR data coverage is presented in Figure 12; there are over 2 million points in the dataset. Points representing elevations above 490 feet were removed from the dataset for development of the hydraulic model because flood elevations considered in this analysis are below elevation 490.

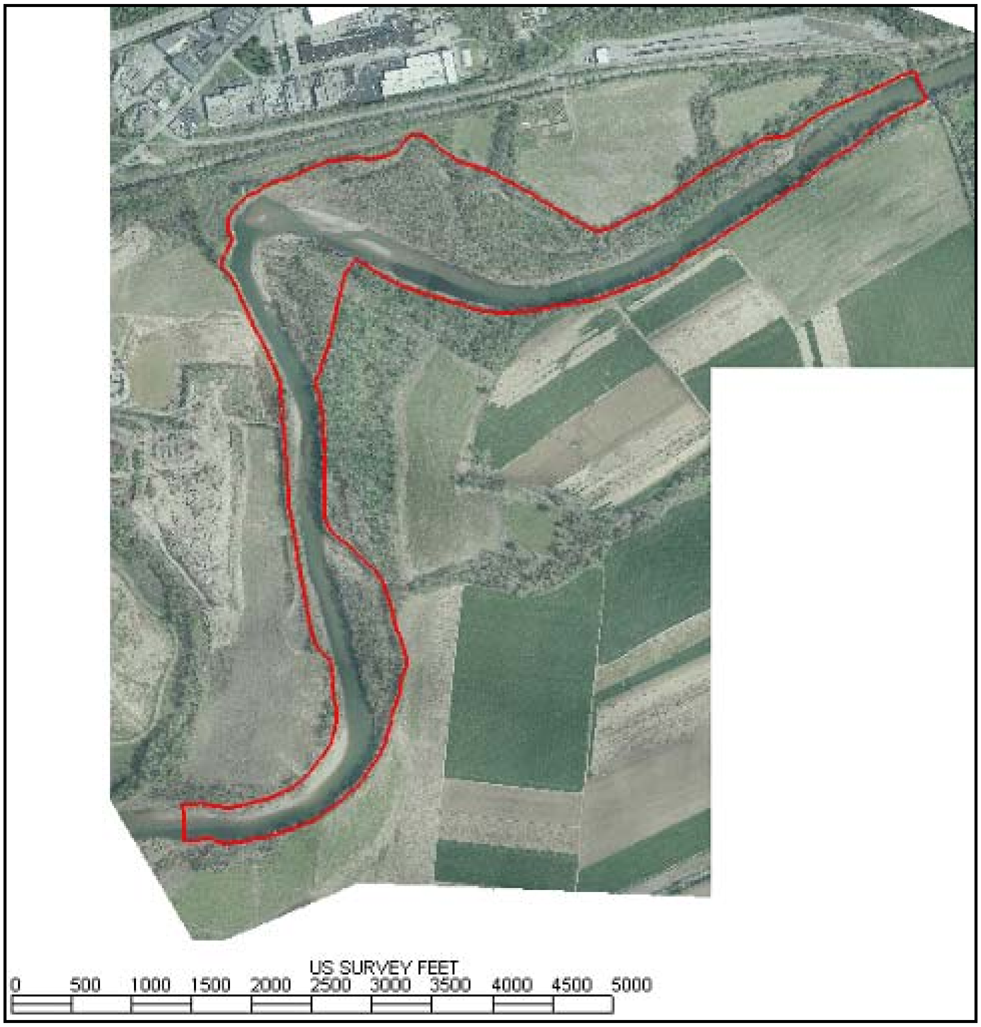

Figure 11: Model grid coverage in the Study Area of the Little Miami River

The field survey data provided bathymetric information not available in the LIDAR dataset, as LIDAR cannot resolve ground elevations below the water surface. The survey dataset contains both a channel thalweg survey and approximately thirty channel cross sections. The locations of the surveyed cross sections are shown in Figure 13, along with the channel thalweg. The two datasets were merged for use in the model, which assigns depths to every node in the model domain.

The high spatial resolution of the LIDAR dataset in relation to the channel bathymetry dataset initially generated problems when the combined dataset was interpolated to the model grid. The interpolation algorithms used by the model provided more weight to the LIDAR data because of the density of the data, and thus the bank elevations represented by the LIDAR data “bled” into the channel in areas where there was not any survey data. This led to unrealistically high channel bed elevations. Figure 14 shows the difference in elevation point density between LIDAR data and the bathymetric survey.

To resolve this issue, HEC-RAS was used to generate interpolated cross sections from those measured during the field survey. Additional bathymetry points were created by interpolation of the existing bathymetry cross sections at 50 foot intervals. Cross section locations were identified with HEC Geo-RAS, and the interpolation of cross sections was done with HEC-RAS. Figure 15 shows the interpolated cross sections in HEC-RAS. Although the cross sections were extended to the entire floodplain, only points between the channel banks were used in the final elevation model. The LIDAR data was used to represent the floodplain in the final model.

Bathymetric cross sections were not available for the two secondary channels that branch in and out of the modeled reaches of the Little Miami River. The low flow condition observed in the LIDAR dataset clearly shows the banks of the two secondary channels. However, it was not clear if those channels were wet or dry at the time of the LIDAR data collection, and if they were wet during data collection, what the depth of water was at the time. For modeling purposes, these secondary channels have minor influence on the primary Little Miami River flows, therefore the LIDAR data was assumed to represent the bottom of the secondary channels. For flows greater than 2000 cfs (the flow at which LIDAR data was collected), the geometry of the side channels is adequately represented by this approach.

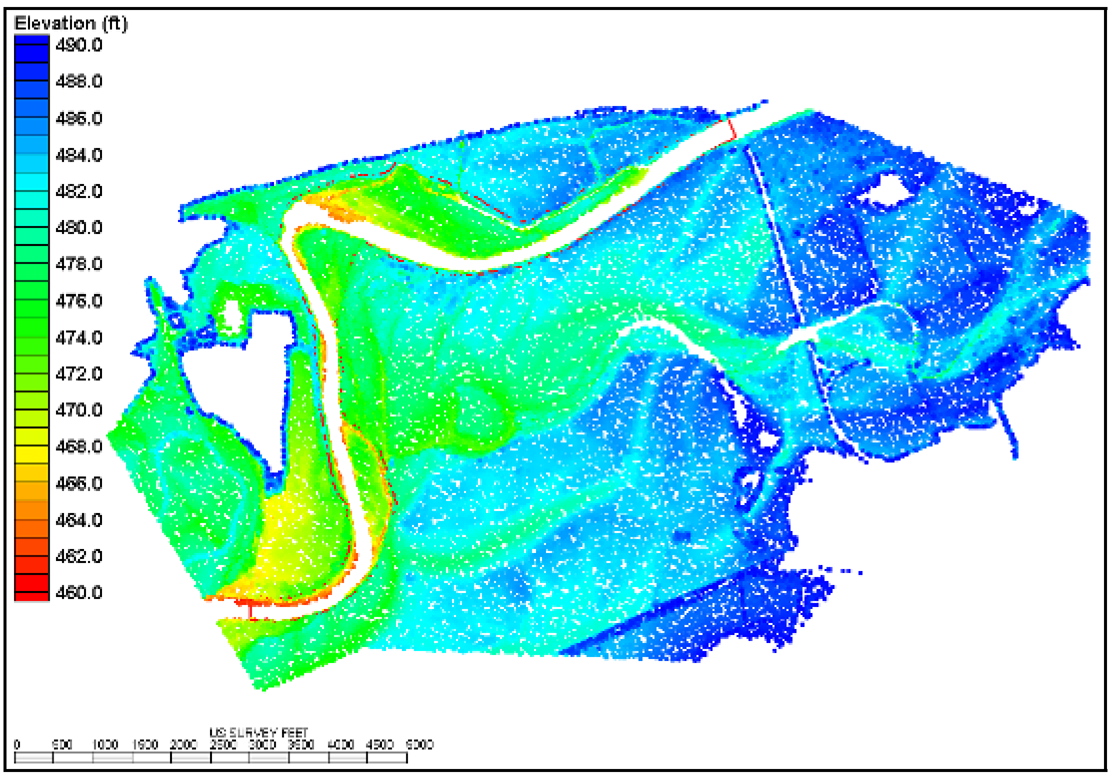

Figure 12: LIDAR data coverage of Study Area

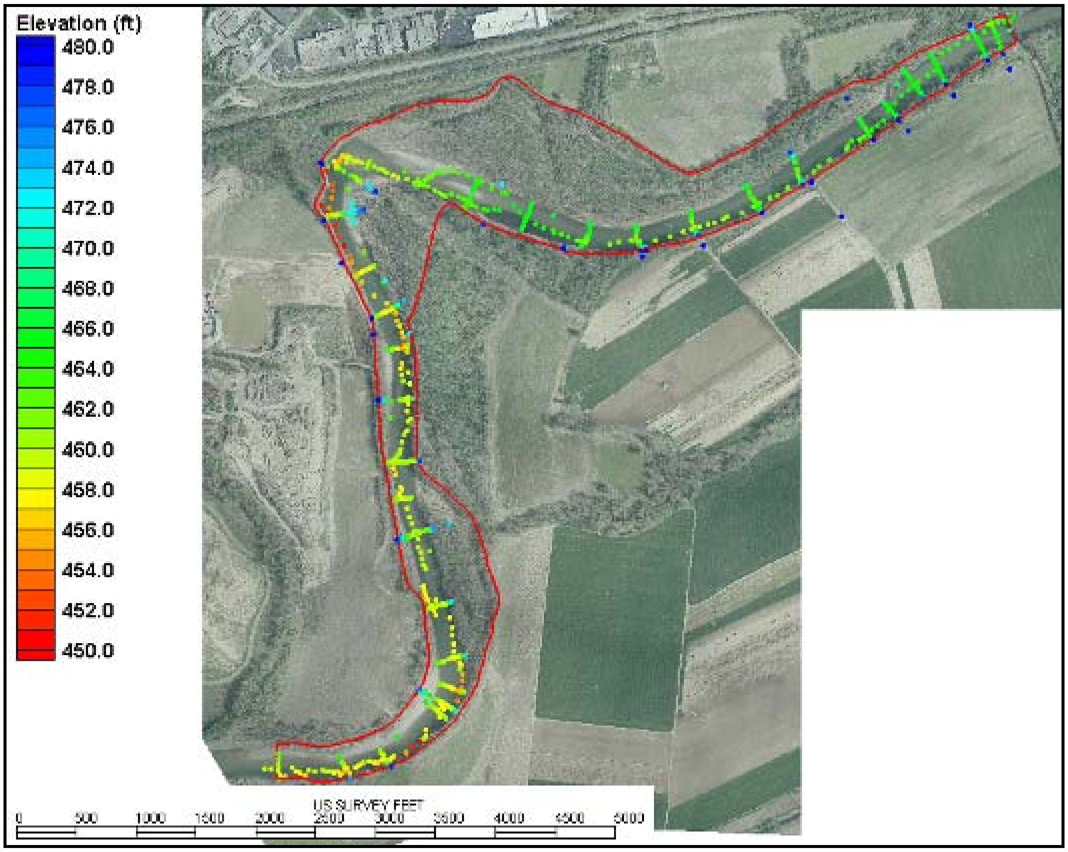

Figure 13: Channel survey of Study Area

Figure 14: Comparison of elevation data density (LIDAR vs. field channel survey)

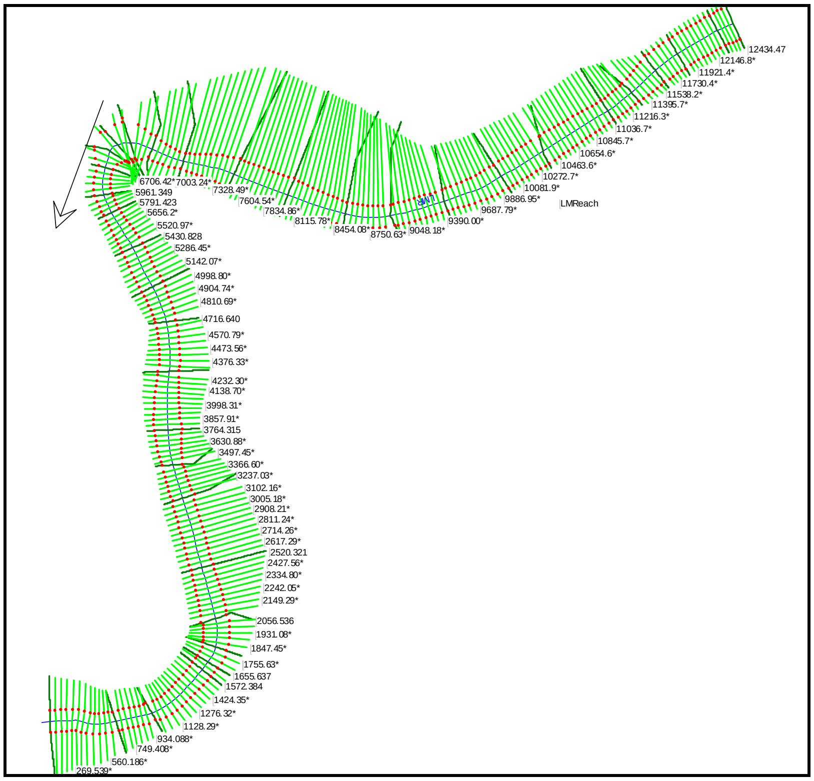

Figure 15: Original (black) and interpolated (green) channel cross sections in HEC-RAS

The two-dimensional hydraulic model grid was constructed in an iterative fashion, with the goal of representing the area inundated by a 45,000 cfs flow (approximately a 3-year flow based on post-1975 hydrology), the largest flow being considered during this phase of analysis. Anecdotal evidence from personnel at the Hamilton County Park District indicates that Otto Armleder Memorial Park is inundated at least once every year, on average, by high flows on the Little Miami River. Therefore, this provides an upper estimate of the likely bankfull or channel forming flow. Further, as described in the hydrologic analysis section, approximately 71% of "downvalley floods" (those likely to cause the greatest channel change) have return intervals of less than or equal to 2 years. Therefore, hydraulic modeling of larger overbank floods is unlikely to provide additional useful information regarding channel stability in the Study Area.

Initial model grids were delineated using the LIDAR data, which effectively shows the lateral extent of the river during discharges of approximately 816 to 2,030 cfs. Flows of increasing magnitude were initially forced through a model grid that likely underestimated the lateral width that high flows would actually inundate. This approach caused a water surface elevation above that expected in the channel for a given flow, since the flow was unrealistically confined to a smaller channel in the model than in the field. To alleviate this problem, the flow depth along the channel banks was analyzed to identify where the high flows would likely spill out of the modeled channel banks. The model was then expanded laterally using this information until the flow depths at the banks no longer indicated that the model was unrealistically confining the flow.

The final model grid consists of 7,982 elements and 20,635 nodes. The average element size is approximately 850 square feet, equal to an average cell with rough dimensions of 30 feet by 30 feet. A portion of the model grid is presented in Figure 16, demonstrating the variability in grid resolution for various portions of the river bed. The model elevation contours are also included in Figure 16. Note the natural sill feature in the main channel that rises approximately five feet from the thalweg elevation upstream of the sill. This could indicate a high deposition area in the channel, and could be related to the lateral spreading of higher flows to the off-channel storage areas to the right of the main channel.

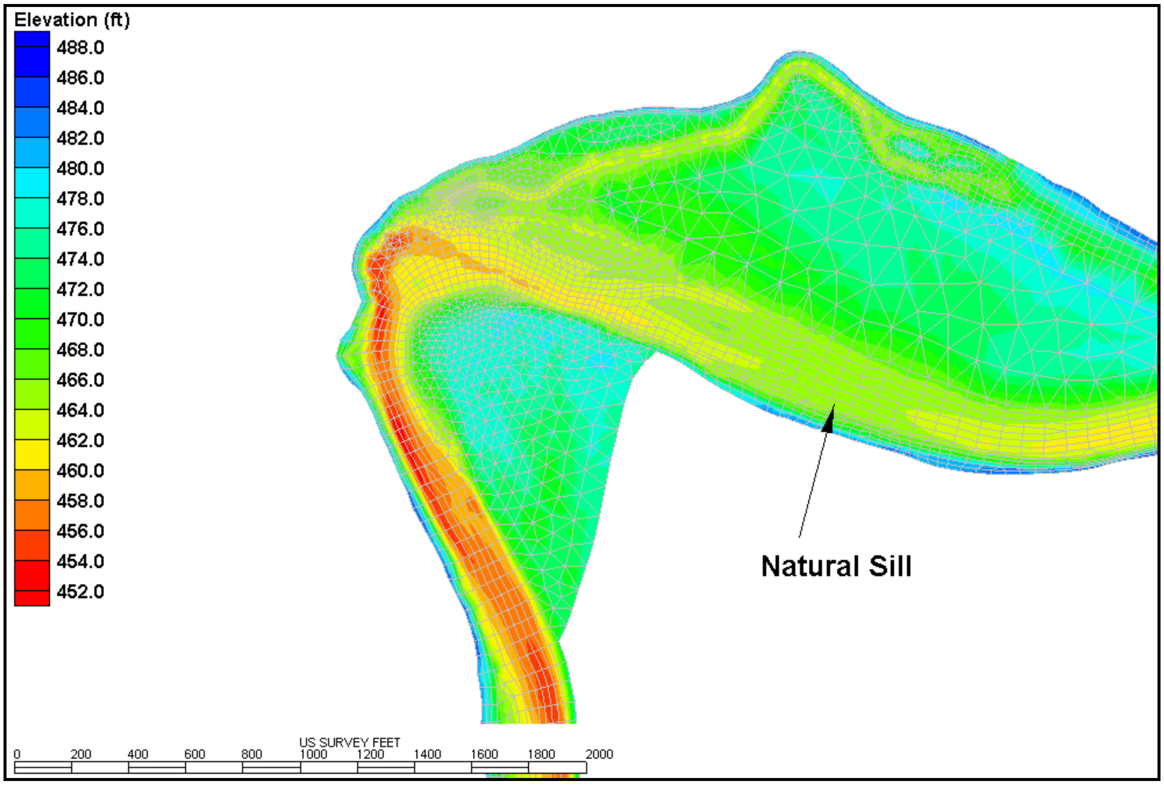

Figure 16: Model grid and elevation contours in geomorphic reach 5 near Horseshoe Bend

Figure 17 presents the distribution of these material types throughout the model domain. The model allows for the specification of bed friction on an element by element basis. Groups of elements representing zones of similar ground cover or channel substrate are assigned identical friction values via a Manning's 'n' value. The Little Miami River model uses five different material types reflecting the varied composition of the channel and floodway, including:

Main channel (n = 0.025)

Side channels (n = 0.035)

Channel bars (n = 0.035)

Channel banks (n = 0.045)

Forested floodway (n = 0.08)

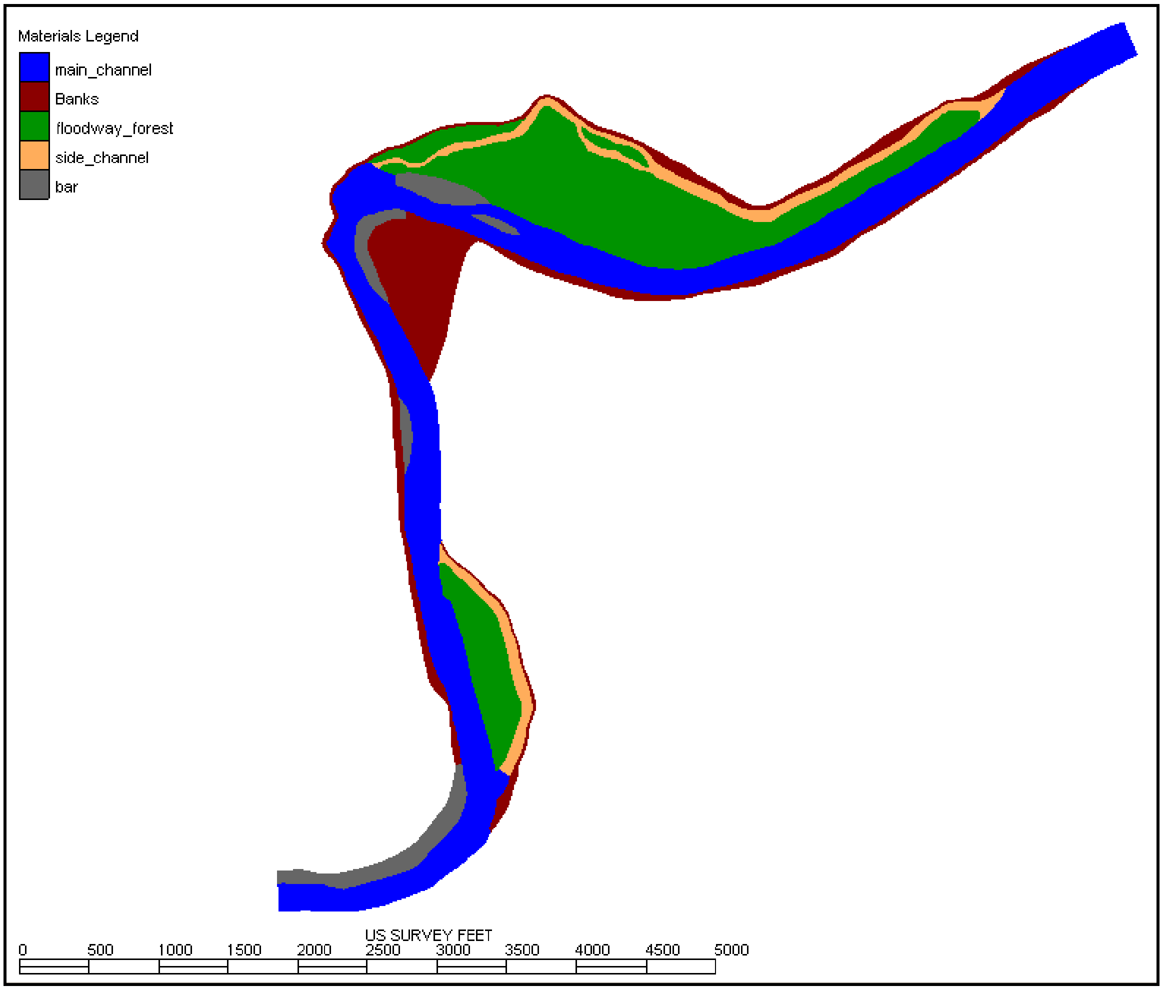

Figure 17: Distribution of channel features (friction map)

5.3 Model Simulations

In this first phase of analysis, model simulations were focused on flows up to and including bankfull for several reasons. First, as the hydrology analysis showed, most of the downvalley floods have return intervals of two years or less. Next, bankfull flow channel hydraulics typically generate the most erosive conditions, as overbank flow energy is dissipated on the floodplain. And last, because no high flow observations are available yet for model calibration, model results for overbank flows would have very high uncertainty. Without the benefit of a stage-discharge curve or other observations to assign the appropriate water surface elevation at the downstream model boundary, a set of simulations was conducted with a range of downstream boundary conditions to bracket likely outcomes. If a high flow event is surveyed during the coming winter months of 2009, the assumed water surface elevations related to high flow events will be verified in Phase 2 of this evaluation.

Model simulations were conducted to represent steady state conditions, and were conducted for a range of flows between 10,000 cfs and 45,000 cfs, representing return intervals up to approximately the two-year flow based on the full period of record hydrology and the three-year flow based on the post-1975 hydrology. Detailed analysis was focused on larger flows representative of bankfull conditions, specifically model simulations of 30,000 cfs, 40,000 cfs, and 45,000 cfs. Figures 18 and 19 present model predictions for water surface elevations at the right and left banks, respectively. Predictions are presented for flows of 30,000 cfs and 40,000 cfs, with two different assumptions for the downstream stage boundary condition to bracket the range of expected conditions. Note that the water surface elevation predictions are not strongly influenced by the specification of the downstream boundary stage. In the examples presented in Figures 18 and 19, a shift in the downstream stage of two feet causes an increase of less than 0.5 feet at a distance of 2000 feet upstream of the downstream model boundary. The comparison of predicted water surface elevations to the adjacent bank elevations indicates that flows as low as 30,000 cfs begin to overtop the channel banks as defined in the model (Figures 11 and 13). This issue will be resolved with another iteration of model grid modifications that will be conducted in Phase 2 after high flow events have been observed and surveyed.

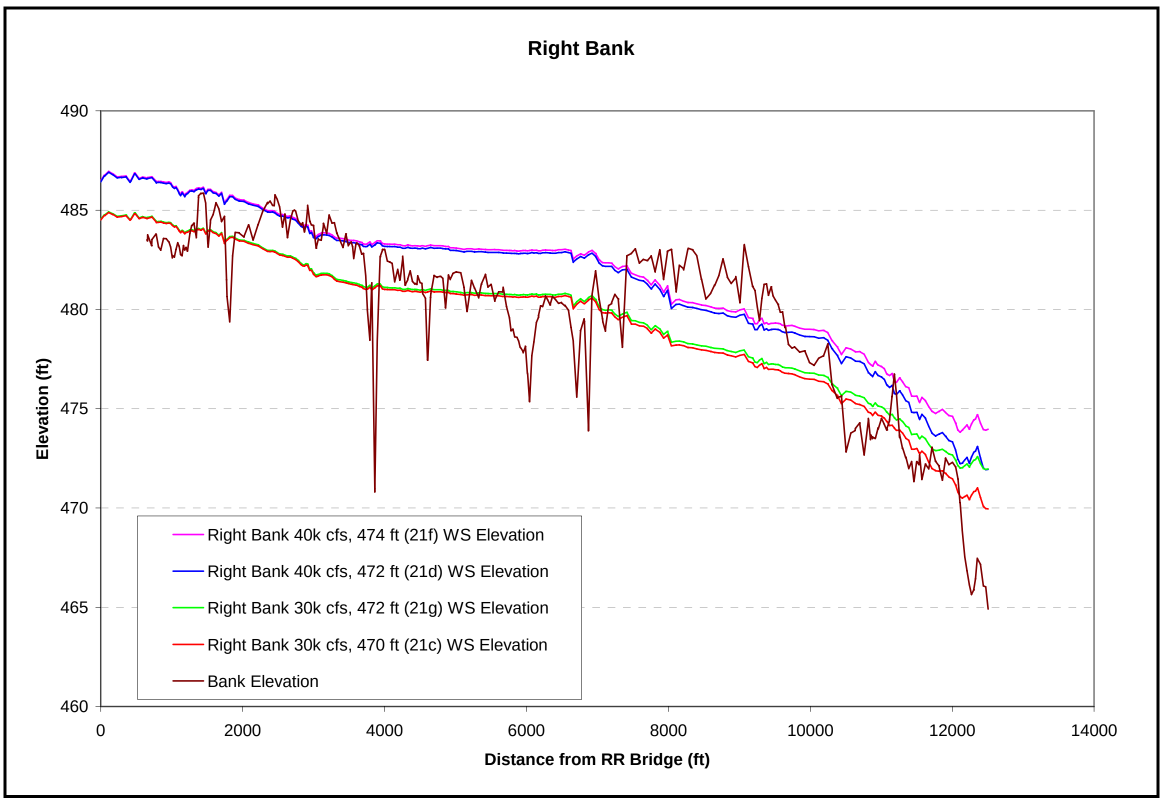

Figure 18: Modeled water surface elevations: 30,000 and 40,000 cfs flows (right bank)

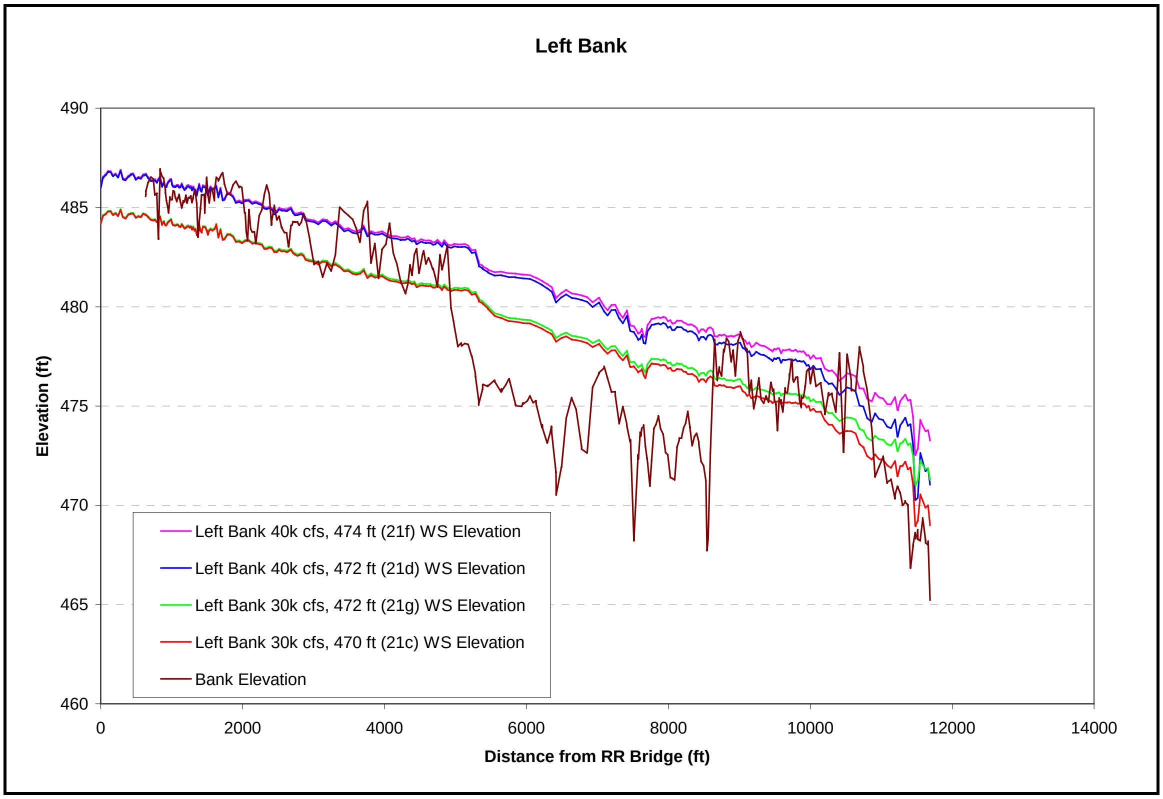

Figure 19: Modeled water surface elevations: 30,000 and 40,000 cfs flows (left bank)

5.4 Model Verification Using HEC-RAS Simulations

A comparison between the preliminary HEC-RAS model and the SMS simulation of the scenario with a flow of 45,000 cfs and a downstream boundary condition of 472 feet is presented in Figure 20. The HEC-RAS simulation used a Manning's coefficient of 0.025 for the main channel and 0.08 for the overbank areas. The cross sections used for the HEC-RAS run and the predicted lateral extent of the water surface are presented in Figure 21. Figure 22 shows the water surface elevation predicted by the two-dimensional model for the same flow and stage conditions.

Model results indicate a difference of up to two feet in water surface elevation between the coarse HEC-RAS model and the refined RMA-2 model. The difference between the model predictions is likely attributable in part to the treatment of overbank areas in HEC-RAS, and the explicit inclusion of the secondary channels in the two-dimensional model. Given this relatively minor difference between the two models, and the lack of high flow observations for model calibration in this phase of evaluation, these results indicate that the multidimensional hydraulic model predictions realistically depict local hydraulics, especially for relative comparisons of geomorphic reaches within the Study Area.

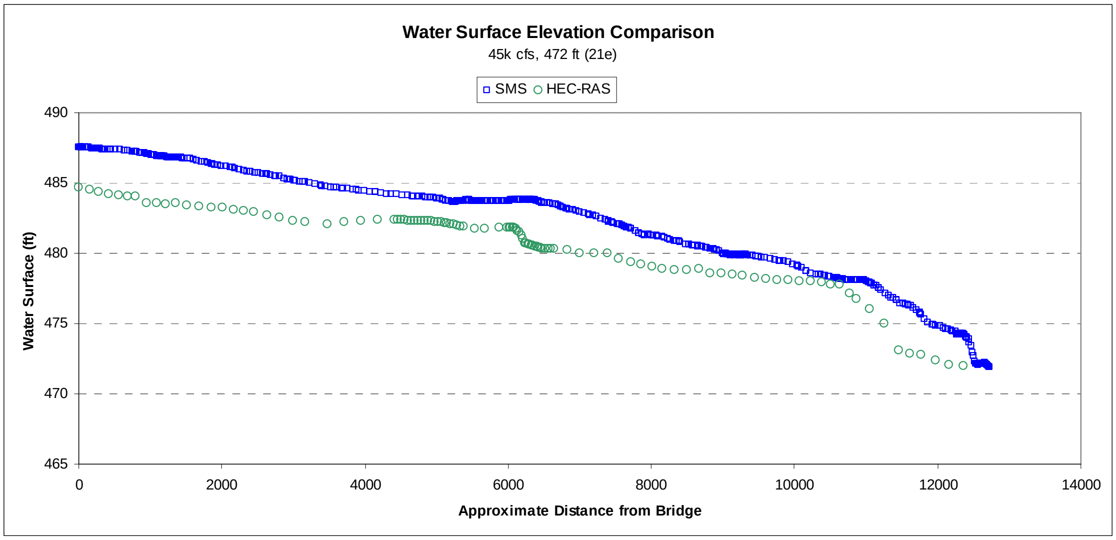

Figure 20: Comparison of HEC-RAS and RMA-2 predicted water surface elevations for 45,000 cfs run with 472 foot downstream boundary condition stage

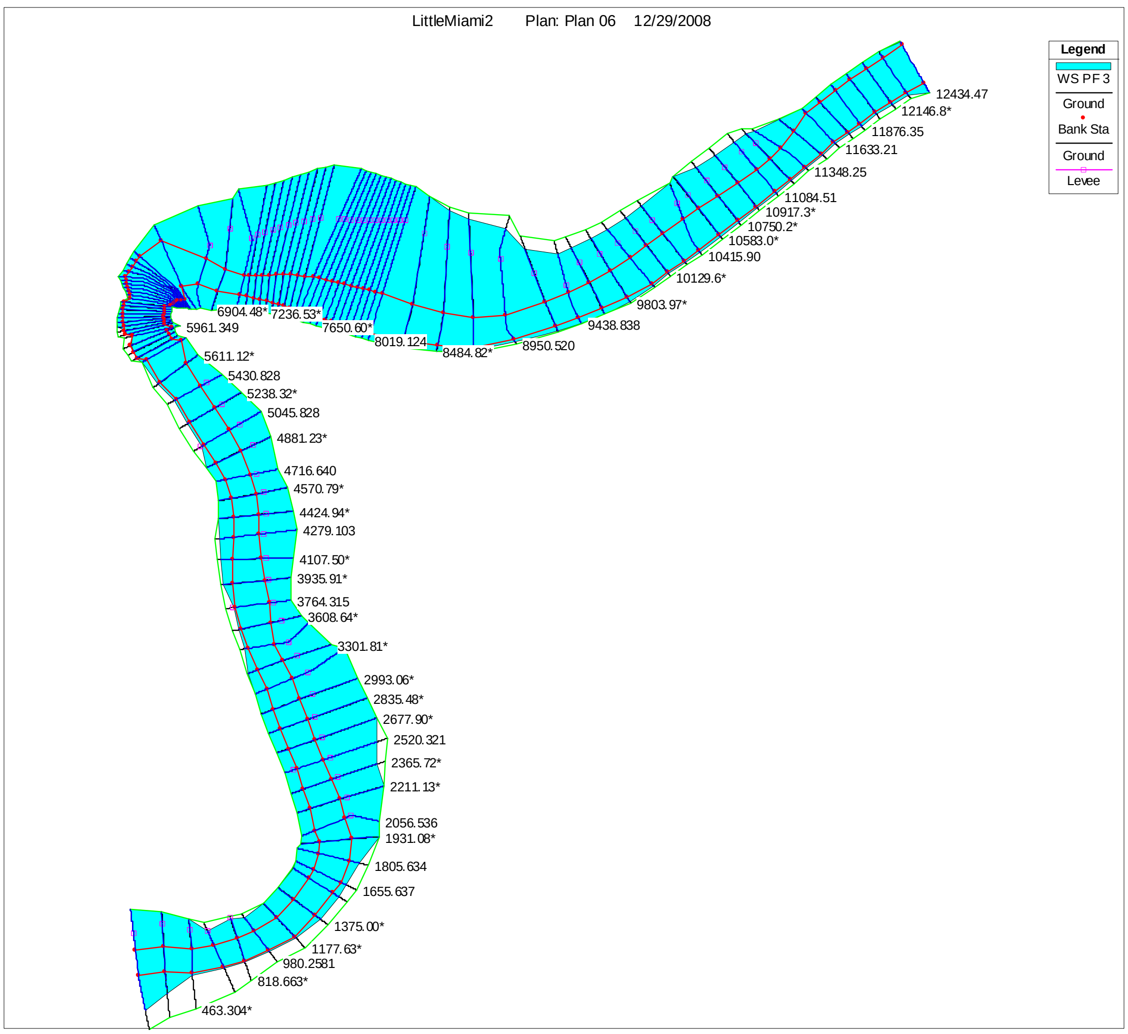

Figure 21: HEC-RAS results for 45,000 cfs run with 472 foot downstream boundary condition stage

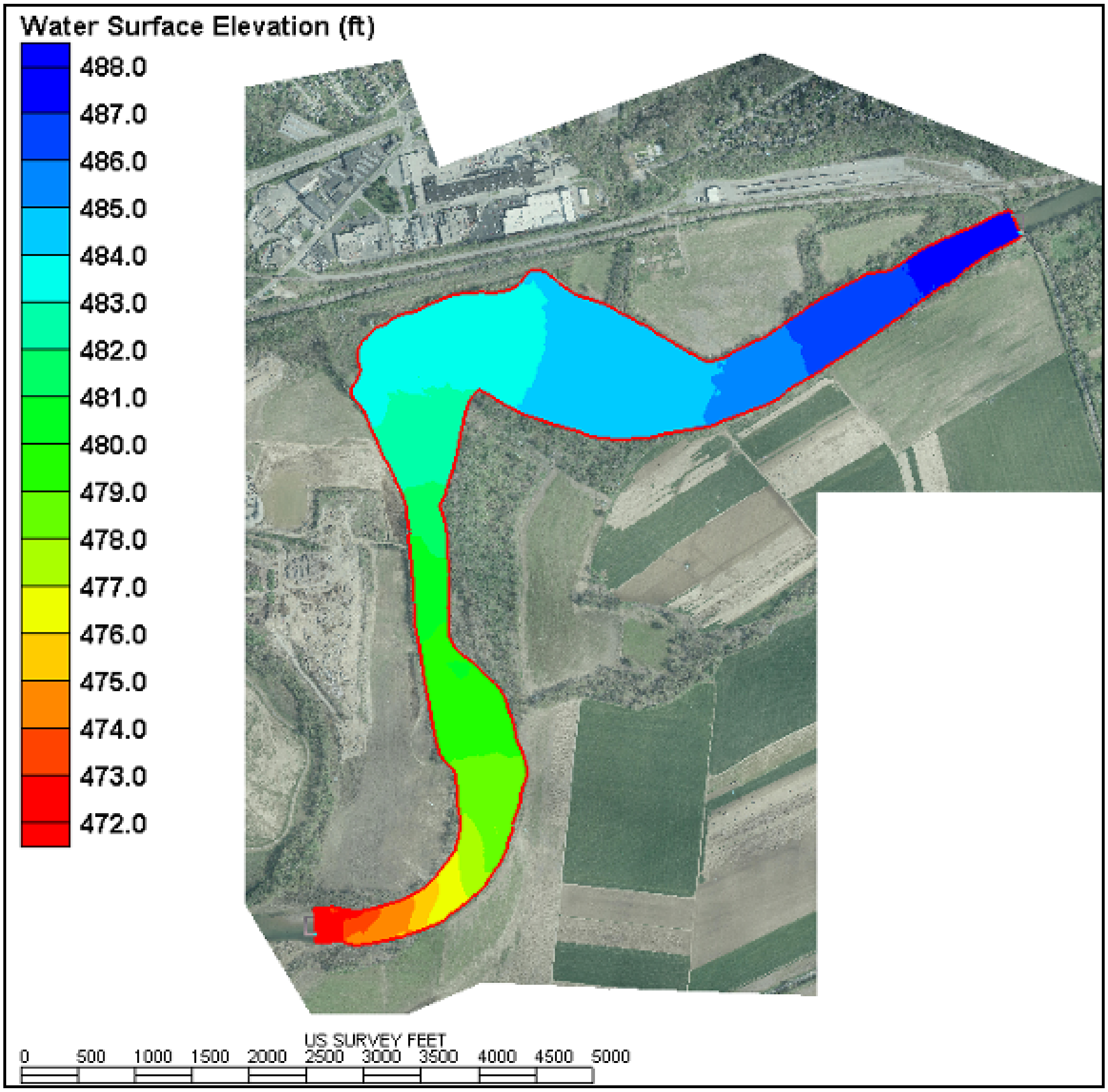

Figure 22: RMA-2 water surface elevation for 45,000 cfs and 472 foot downstream stage

5.5 Model Guidance on Suitability of Geomorphic Reaches for Clear Span Bridge Crossing

The Phase 1 hydraulic model results can be used to further refine evaluation of the geomorphic reaches in the Little Miami River with respect to their likely future stability, and therefore their suitability for a clear span bridge crossing. Predicted model velocities and water surface elevations provide information on the inundation areas for various flows and identify areas with local erosion and deposition concerns where channel evolution is likely in the future. Longitudinal velocity transects are presented in Figure 23 for simulations with 30,000 cfs, 40,000 cfs, and 45,000 cfs. The four proposed clear span bridge crossings are indicated on the chart with vertical lines at their approximate locations. These velocity predictions are for the channel thalweg, the deepest part of the channel but not necessarily the channel center. Model results indicate that channel thalweg velocities are lowest in the vicinity of Horseshoe Bend (geomorphic reach 5) and highest at the two proposed downstream crossing locations (geomorphic reaches 6 and 7). Flow velocities drop significantly at Horseshoe Bend because of the sharp meander bend in the channel and the extensive area of overbank flow across the large point bar on the inside of the channel bend. As shown in the historical channel morphology analysis, this is a highly active area of the river, which is supported by the hydraulic model results showing complex flow patterns across the point bar and through the meander bend.

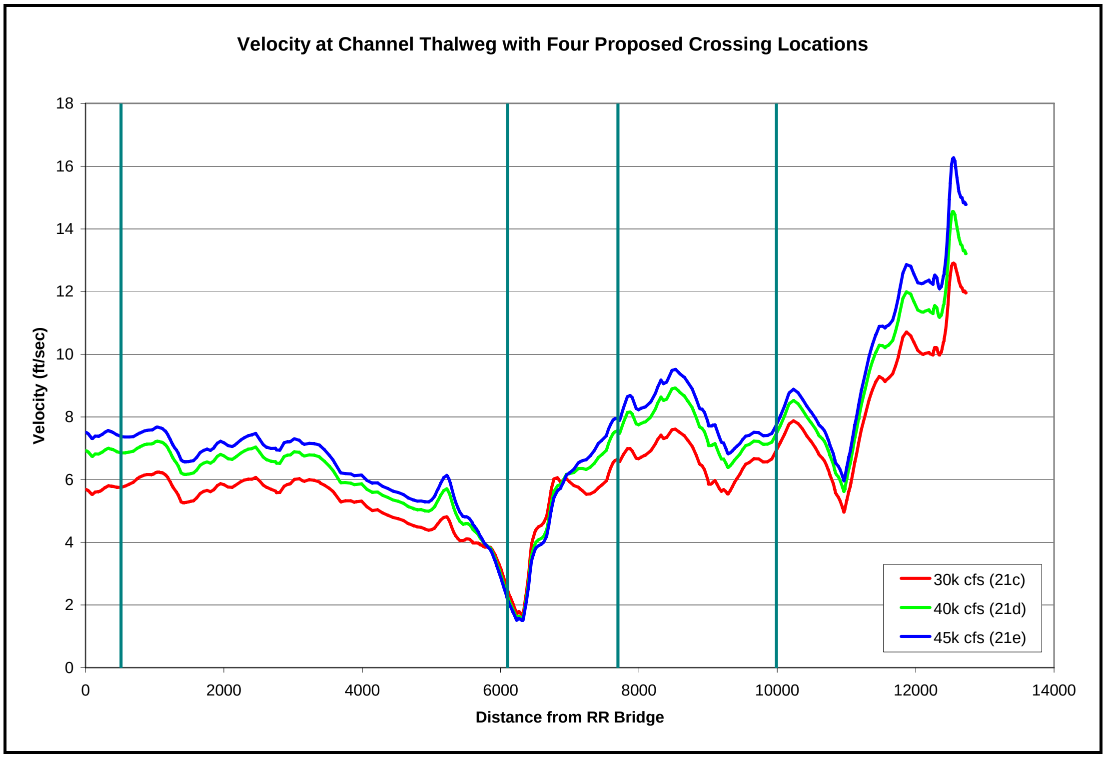

Figure 23: Comparison of channel thalweg velocity predictions from 2D model

One major benefit of this multi-dimensional modeling effort with respect to characterizing suitability of different geomorphic reaches for a clear span bridge crossing is the ability of the model to provide information on the lateral variations in the flow field. This is a distinct improvement over hydraulic predictions from one-dimensional models, and provides a predictive capability not possible from observations of current or historical channel conditions alone.

To visualize the model predictions within geomorphic reaches, model results were output in linear transects near each proposed crossing location in geomorphic reaches 4, 5, and 7, and in the middle of geomorphic reach 6. Figures 24 through 27 present these cross-section velocity profiles for flows of 30,000 cfs, 40,000 cfs, and 45,000 cfs. The bathymetric cross section for each transect is included in each figure for reference. Figure 24 presents velocity transects near the upstream most proposed crossing location in geomorphic reach 4. Conditions are very uniform throughout the section, with slightly reduced velocities along the right bank. Peak centerline velocities are approximately 7.4 ft/sec for the 45,000 cfs flow at this cross section. While peak velocities are relatively high in this geomorphic reach, the uniformity of velocity across the channel likely contributes to the relative stability of this reach documented in the historical channel morphology analysis.

Velocity transects at the proposed Horseshoe Bend crossing location in geomorphic Reach 5 are presented in Figure 25. Note that the highest flow velocities (6.4 ft/sec) occur on the shallow left overbank areas, where flow spills over the shallow point bar on the inside of the meander bend. Predicted velocities drop to just over 1 ft/sec along the outside of the meander bend. These complex hydraulics are typical of migrating meander bends and generally promote ongoing meander migration through either point bar deposition and outside bend bank erosion or channel cutoff. Therefore, this geomorphic reach is likely to remain unstable as it has been historically. Figure 26 shows the model predictions near the proposed crossing location just downstream of Horseshoe Bend in geomorphic reach 5. Peak velocities for the 45,000 cfs simulation are 8.2 ft/sec, and there are significant velocity gradients across the section. While not as extreme as conditions in the Horseshoe Bend, these gradients indicate that this location is also likely to be somewhat unstable in the future.

Velocity transects near the center of geomorphic reach 6 are presented in Figure 27. Velocity is relatively uniform across the channel in this location, with lower velocities near the channel banks. Velocity patterns vary somewhat at the upstream and downstream ends of this geomorphic reach as it transitions out of and into the upstream and downstream geomorphic reaches. Model predicted velocity transects for the downstream-most proposed crossing location in geomorphic reach 7 are presented in Figure 28. Peak velocities in the main channel are 7.9 ft/sec, and velocity gradients are similar to those near proposed crossing 3, with centerline velocities considerably higher than bank velocities. Velocities vary significantly in the secondary channel and across the bar at this transect, creating relatively complex hydraulic conditions in this reach.

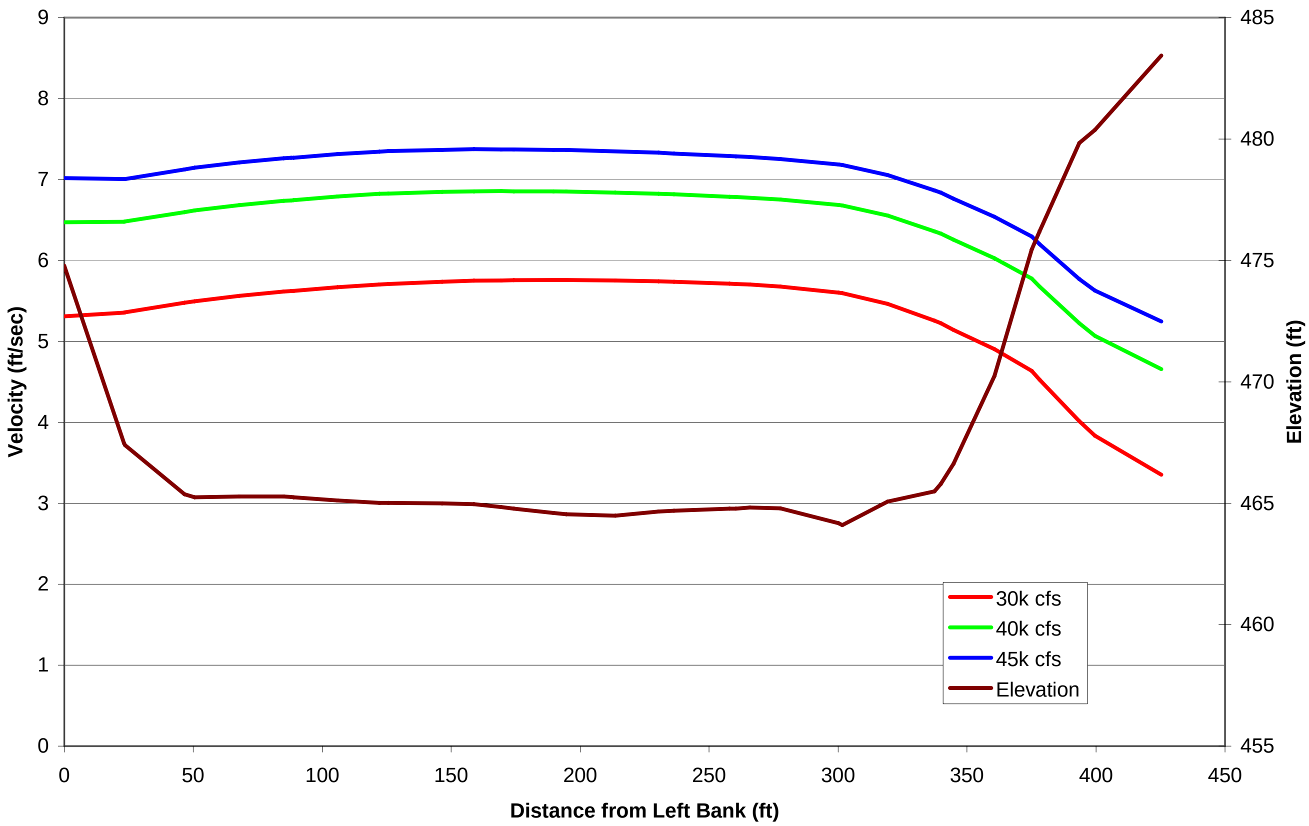

Figure 24: Comparison of cross section velocities for a range of high flows near most upstream proposed crossing location in geomorphic reach 4

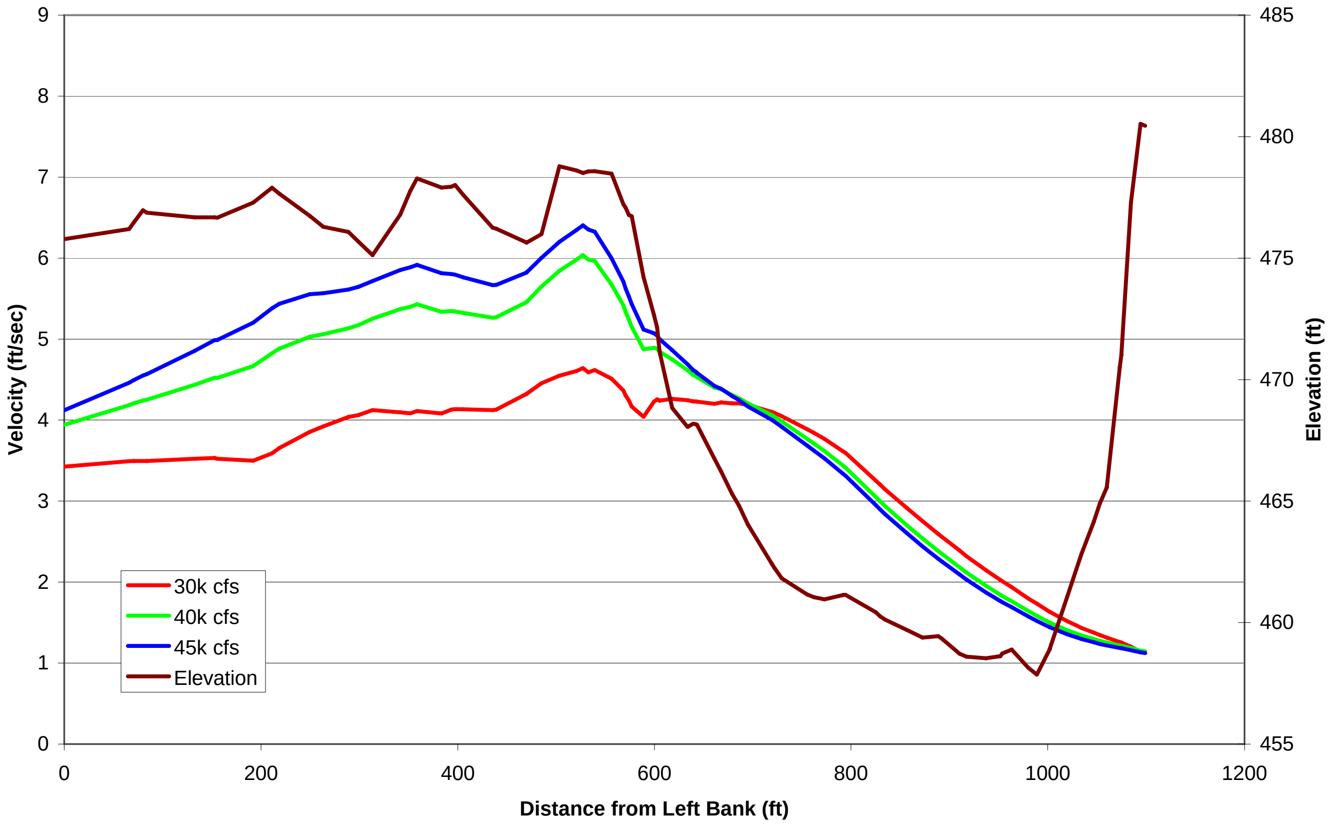

Figure 25: Comparison of cross section velocities for a range of high flows near proposed "Horseshoe Bend" crossing location in geomorphic reach 5

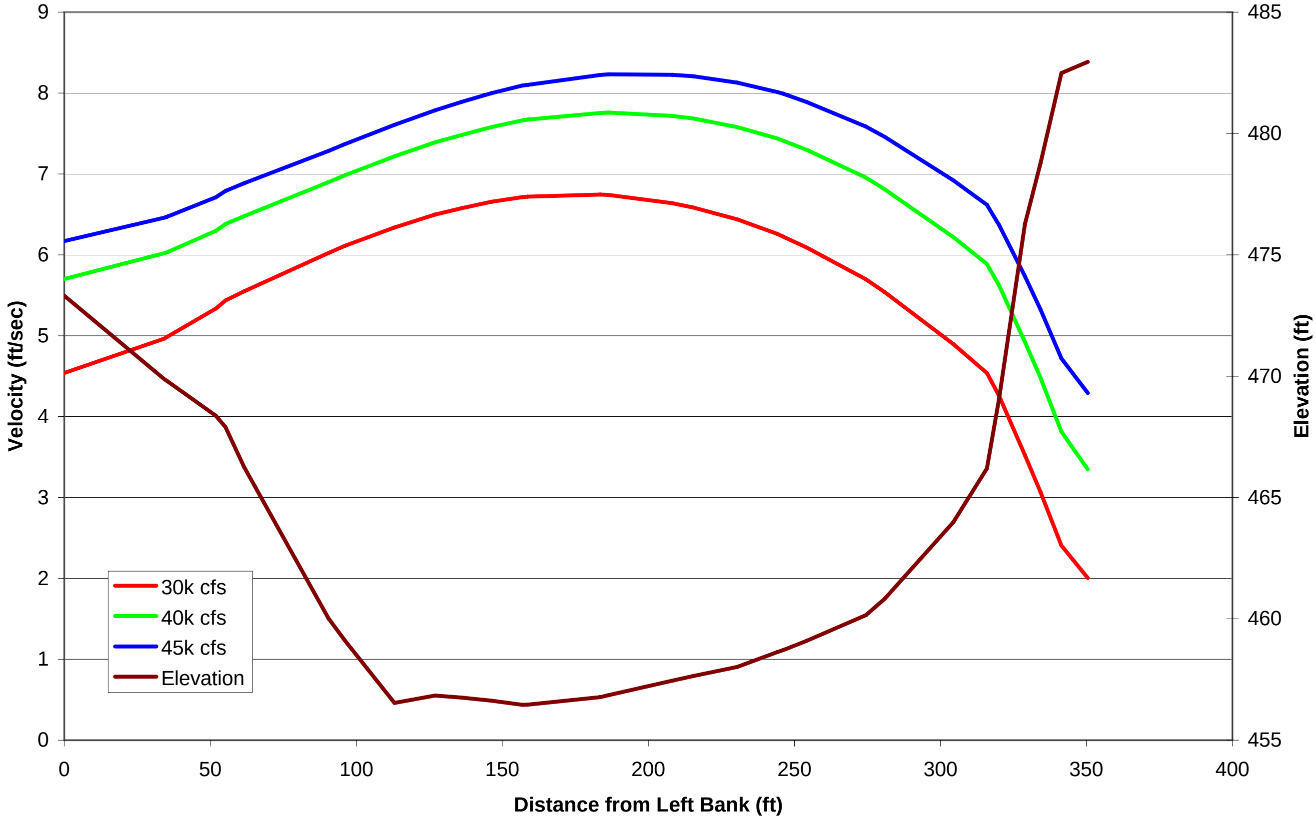

Figure 26: Comparison of cross section velocities for a range of high flows near proposed crossing location downstream of the "Horseshoe Bend" in geomorphic reach 5

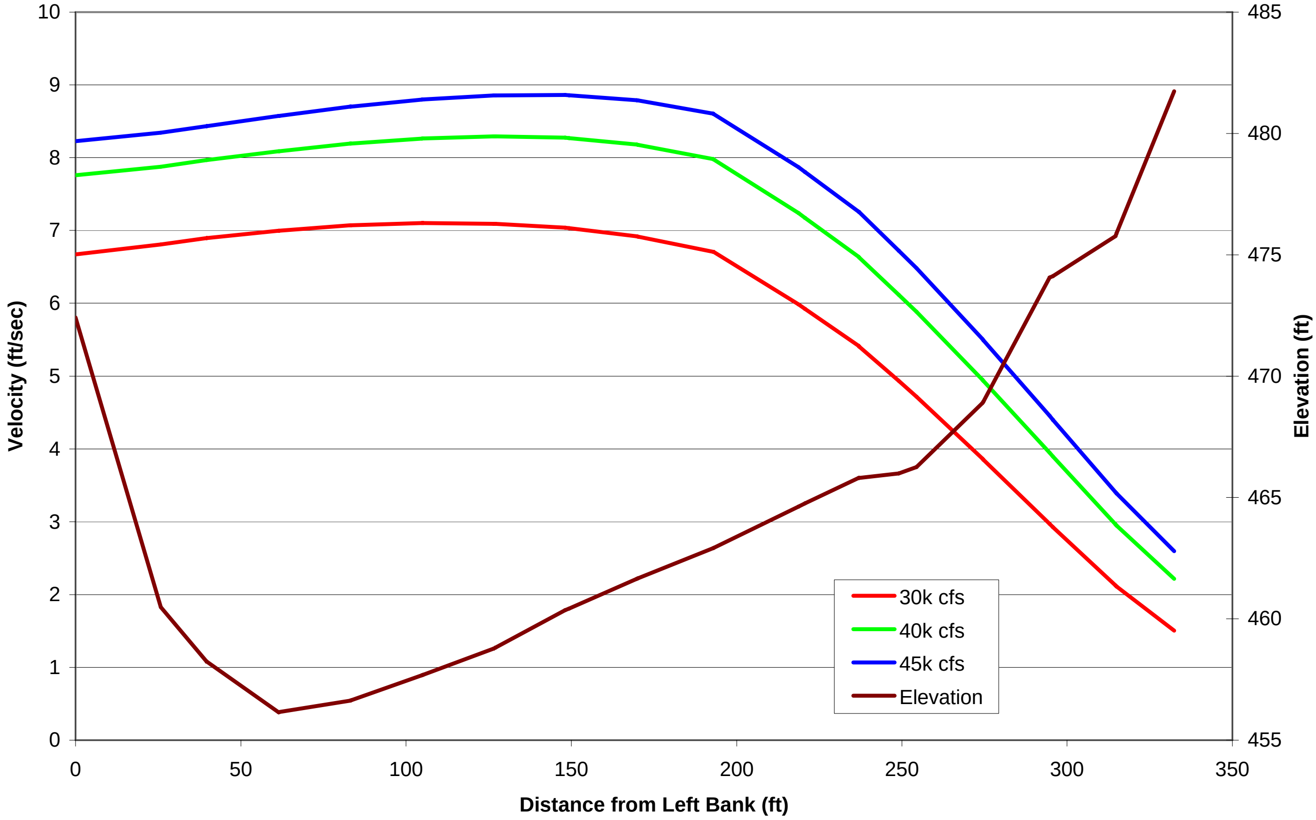

Figure 27: Comparison of cross section velocities for a range of high flows in geomorphic reach 6

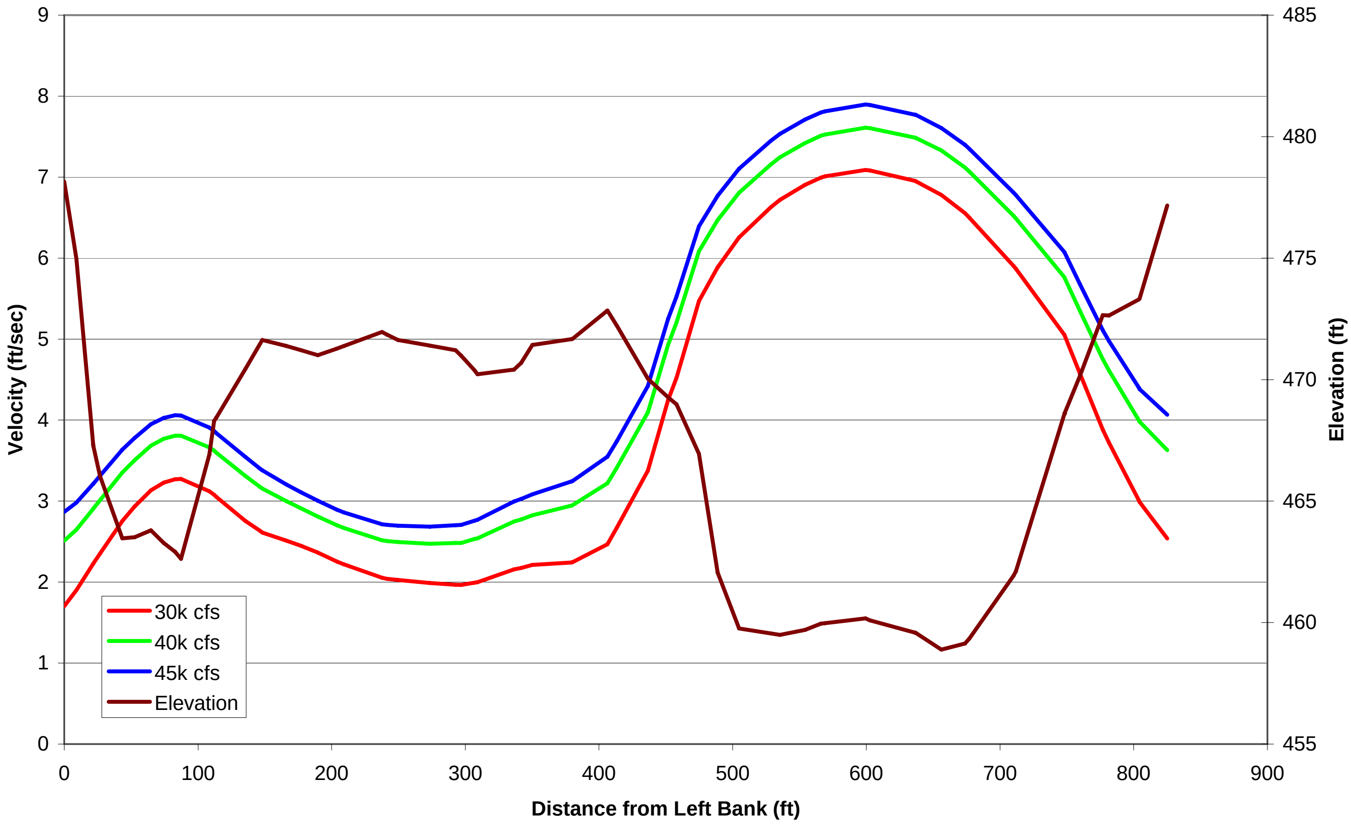

Figure 28: Comparison of cross section velocities for a range of high flows near most downstream crossing location in geomorphic reach 7

Plots of flow vectors are presented in Figures 29 to 32. These plots illustrate hydraulic conditions in each of the four geomorphic reaches in the Study Area. Figure 29 shows the straight, uniform velocity vectors in geomorphic reach 4. Hydraulic model results in this reach support the conclusion of the historical channel morphology analysis that this reach has been and is likely to remain relatively stable. In Figure 30, the focusing of flow around Horseshoe Bend in geomorphic reach 5 is clearly visible. The modeled flow of 45,000 cfs has overtopped the point bar on the inside of the meander bend and is short-cutting the bend along the left bank. Further, flow vectors along the outside of this meander bend are generally pointed directly at the face of the outside bank and diverge and converge through the meander bend. For slightly lower flows that are confined within the channel in this reach, the velocity vectors will be higher than those presented in Figure 30. These local hydraulic predictions strongly suggest that continued channel change is likely in this geomorphic reach.

Conditions at the proposed crossing location downstream of the Horseshoe Bend are also presented in Figure 30, again showing a focusing of the flow where the channel narrows as it exits Horseshoe Bend. This portion of geomorphic reach 5 has elevated velocities primarily due to confinement of the channel width. Figure 31 illustrates the uniform flow vectors present in most of geomorphic reach 6 as well as the converging and diverging flow vectors at the upstream and downstream ends of the reach that could contribute to instability in the reach over the long term. Finally, conditions in geomorphic reach 7 near the most downstream proposed crossing location are presented in Figure 32. Velocity vectors are generally parallel in this reach, and magnitudes are slightly lower than those in geomorphic reach 5 because of the additional flow width in this section of the river.

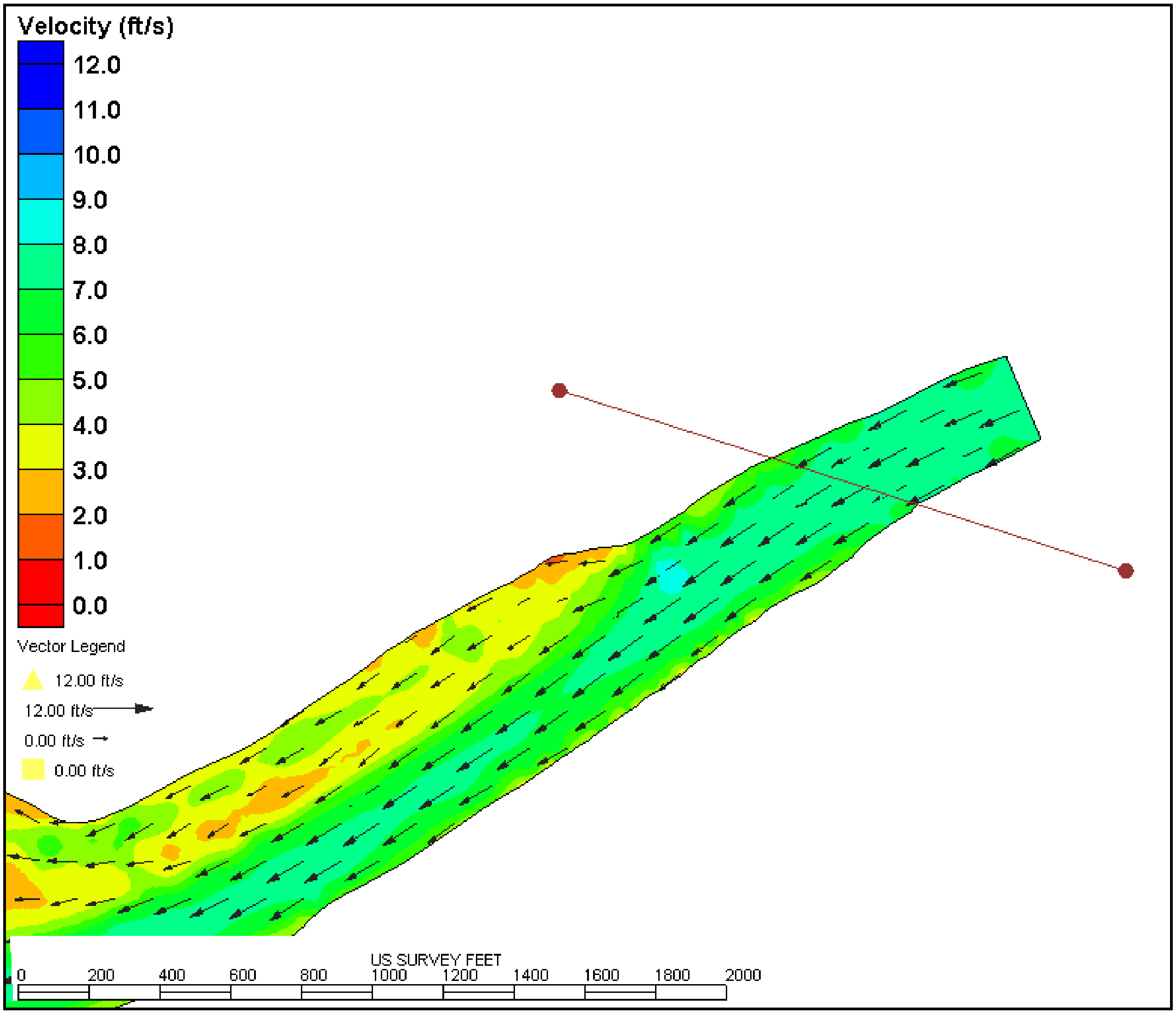

Figure 29: Modeled velocity vectors for 45,000 cfs flow in geomorphic reach 4 (includes most upstream proposed crossing location)

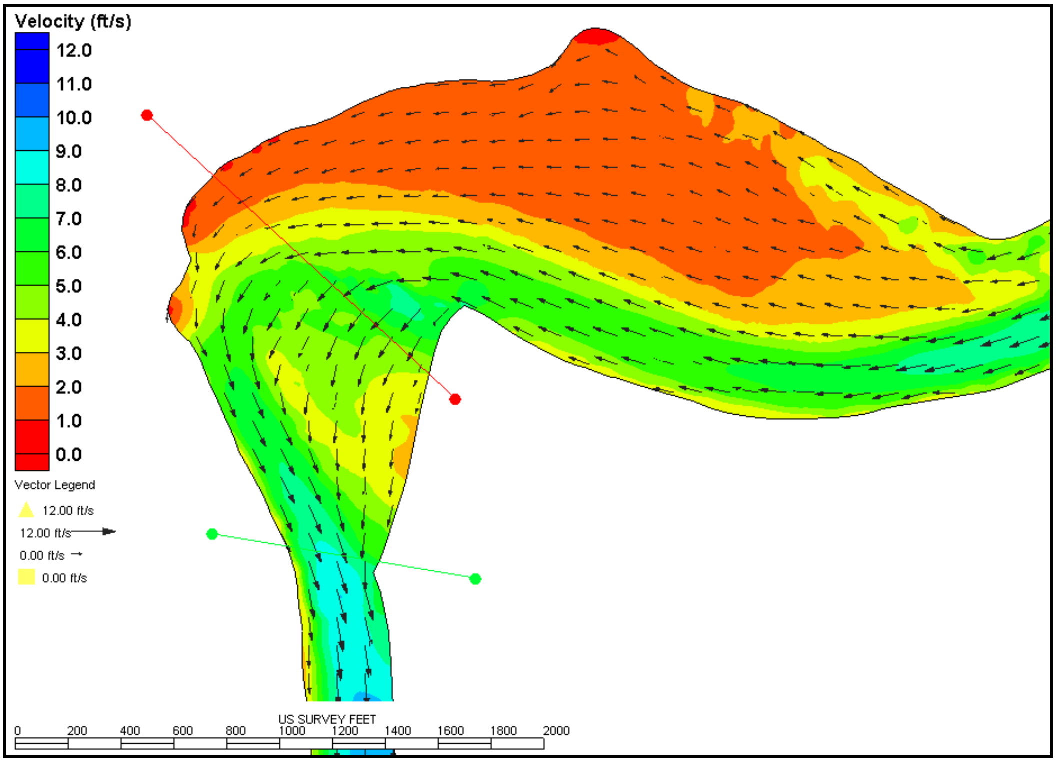

Figure 30: Modeled velocity vectors for 45,000 cfs flow in geomorphic reach 5 (includes proposed cross location at and just downstream of Horseshoe Bend)

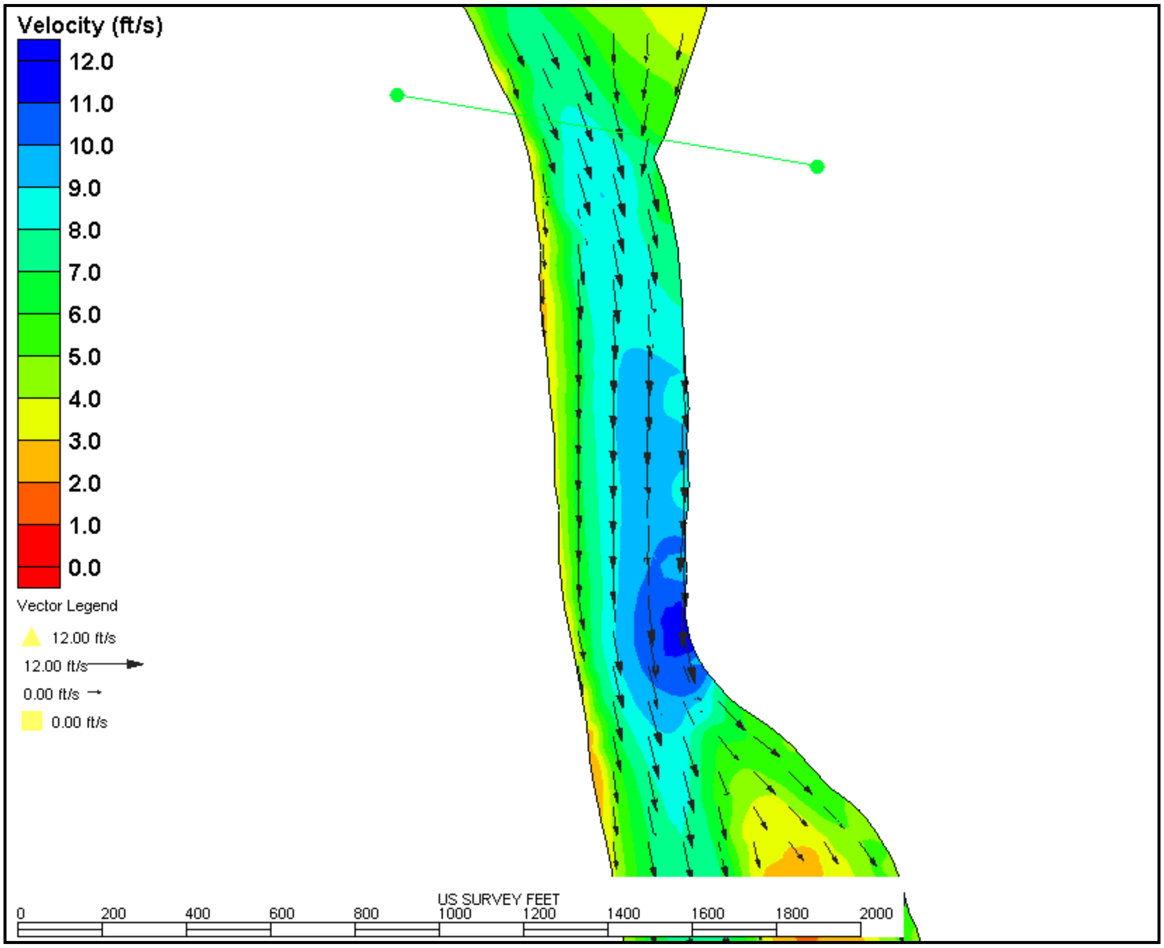

Figure 31: Modeled velocity vectors for 45,000 cfs flow in geomorphic reach 6

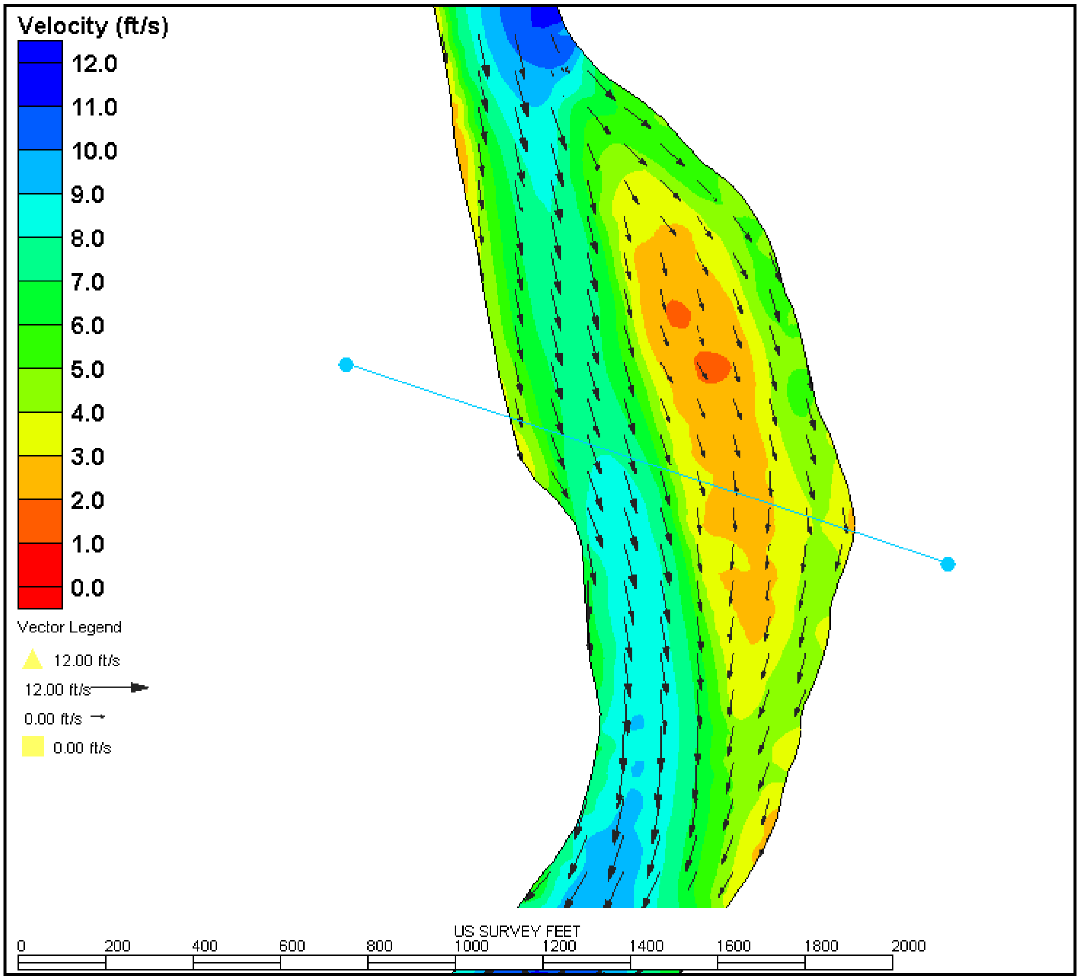

Figure 32: Modeled velocity vectors for 45,000 cfs flow in geomorphic reach 7 (includes most downstream proposed crossing location)

5.6 Sediment Transport Simulations

Preliminary sediment transport simulations were conducted to determine likely erosional and depositional areas within the Study Area at bankfull flows. Because no high flow observations were possible in this phase of the evaluation, this preliminary sediment transport evaluation focuses on predicted bed shear values as indicators of likely erosion or deposition in the Study Area. This information is useful in the initial evaluation of the suitability of each geomorphic reach for a clear span bridge crossing. The sediment transport simulations will be refined in Phase 2 to evaluate site specific sediment transport characteristics at the remaining proposed crossing locations.

Figure 33 presents the predicted distribution of bed shear for a flow of 45,000 cfs. The shear near the most upstream proposed crossing location in geomorphic reach 4 is slightly lower than that near the proposed crossings locations at and immediately downstream of the Horseshoe Bend in geomorphic reach 5. The predicted bed shear in both of these reaches indicates that they have potential erosive areas under high flow conditions. However, in the primary channel in geomorphic reach 5, the bed shear is considerably lower and therefore indicative of potential deposition in areas of shallow overbank flow. This spatial variability

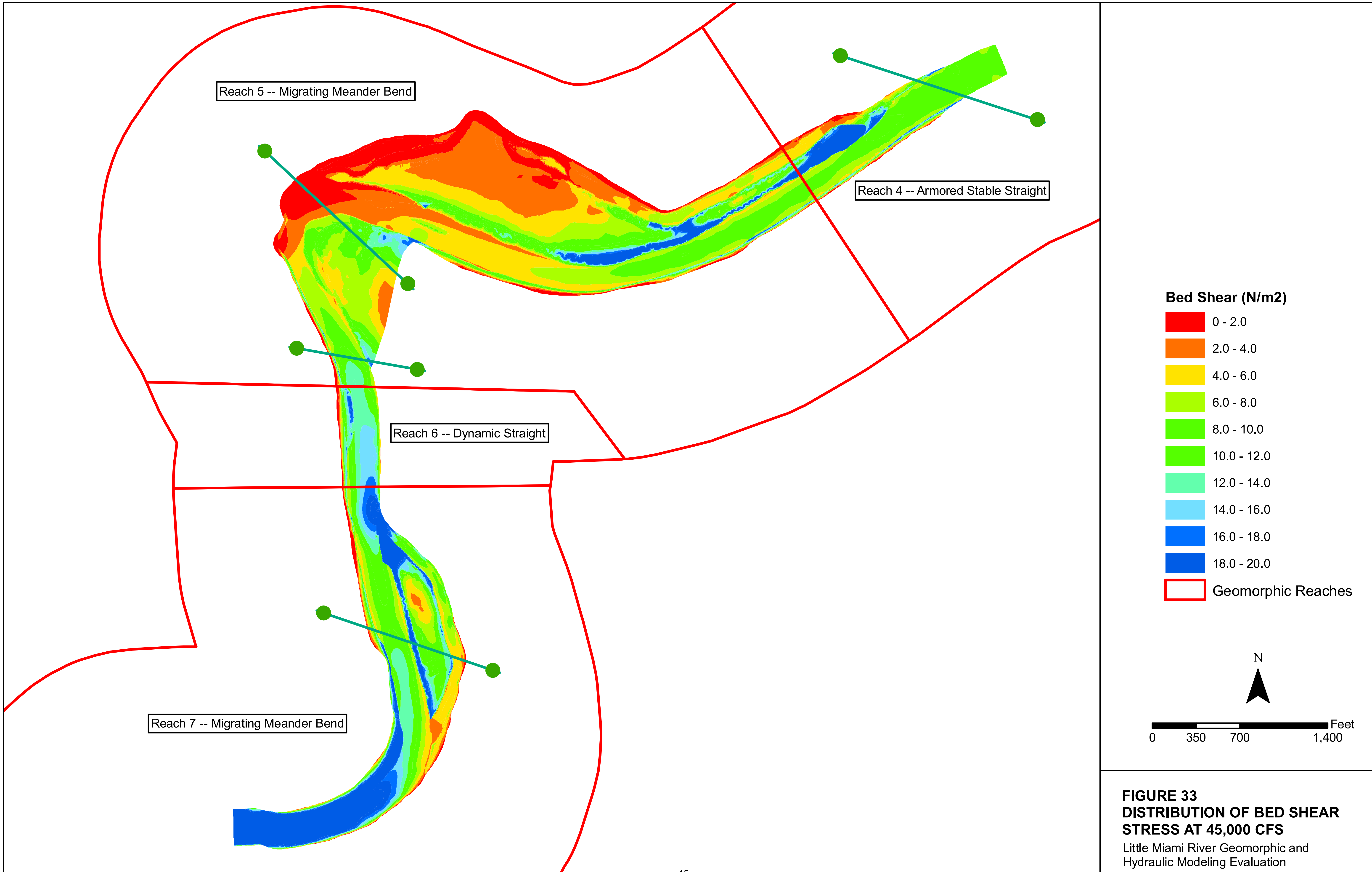

FIGURE 33
DISTRIBUTION OF BED SHEAR STRESS AT 45,000 CFS

Little Miami River Geomorphic and Hydraulic Modeling Evaluation

\\SFO31029951\PROJECTS\LITTLEMIAMIRIVER\GIS\MAPFILES\SHEARSTRESS.MXD SHEARSTRESS.MXD AFALZONE 1/25/2009 23:29:41

of bed shear drives the ongoing channel evolution in this reach and is the primary reason that this geomorphic reach is likely to continue to evolve in the future. It is important to note that these model predictions are for overbank flows in the vicinity of Horseshoe Bend (Figure 34). For smaller flows completely contained between the right bank and left bank point bar, the velocity vectors and shear predictions indicate potential erosion along the outside of the meander.

The bed shear in geomorphic reach 6 is relatively high due to lateral channel confinement but exhibits relatively little spatial variability, similar to bed shear conditions in geomorphic reach 4. Bed shear in geomorphic reach 7 is spatially variable because of the secondary channel and associated topographic complexity along the left bank. Combined with the relatively high bed shear values in this reach, it is likely that this geomorphic reach will continue to evolve in the future as well.

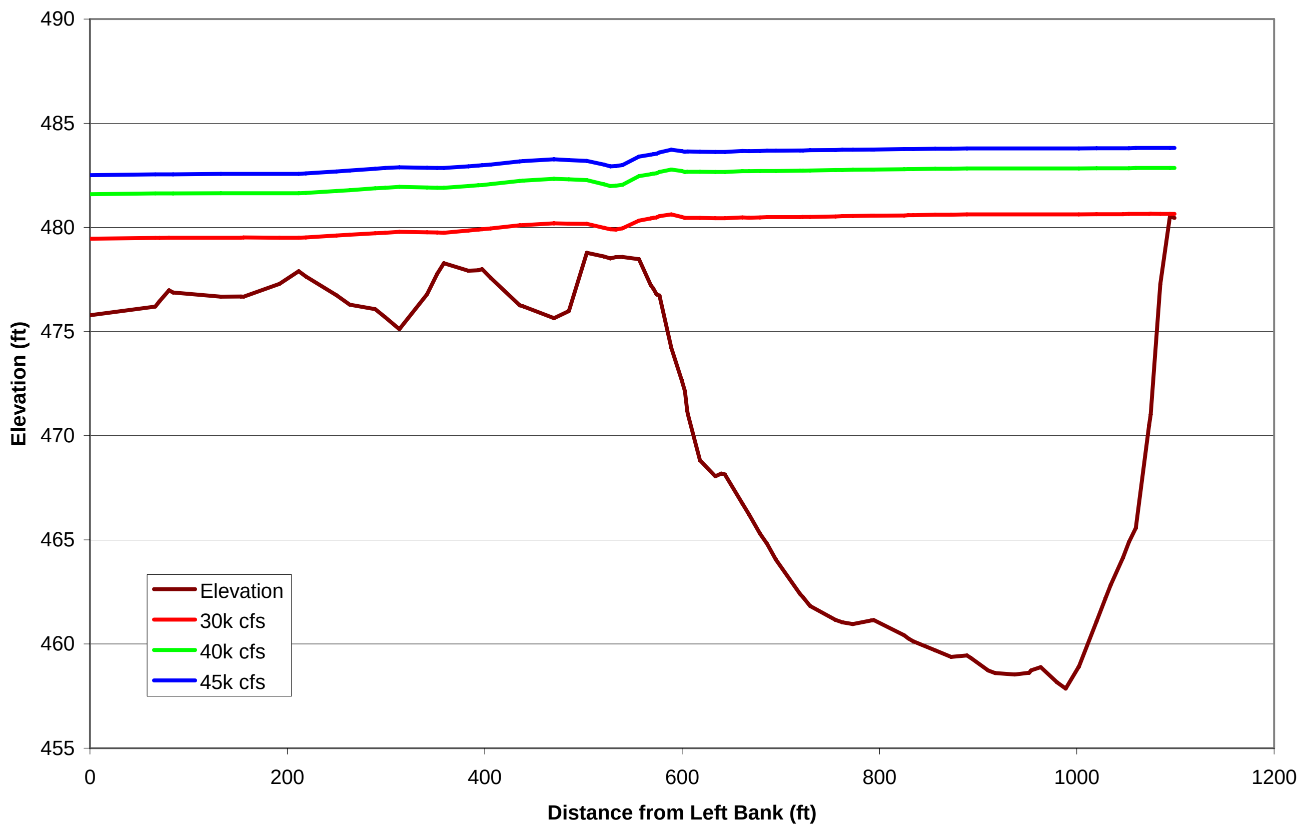

Figure 34: Water surface elevations predicted by the 2D hydraulic model in geomorphic reach 5 at the Horseshoe Bend showing the shallow flow over the large point bar on the left bank

6 Suitability Assessment of Geomorphic Reaches for Clear-Span Bridge Crossing

Table 4 summarizes key results from this analysis relative to the suitability of each geomorphic reach for a clear span bridge crossing. The average annual migration rate listed in Table 4 is the average of the long-term channel migration rates for the right and left banks at the location of maximum long-term average migration in each geomorphic reach (see Table 3 for data used to produce this value). Based on the analyses summarized in the preceding sections, geomorphic reach 5 has very low suitability for a clear span bridge crossing because of its historical instability, its high average lateral migration rate, the presence of complex channel forms and secondary channel influences, and its hydraulic and sediment transport characteristics that are highly conducive to significant future channel change. While geomorphic reach 6 has the second lowest long-term average and short-term maximum annual migration rates, the potential for a meander cutoff at the Horseshoe Bend meander upstream and associated major channel change in this reach is too high to rule out and would make designing a bridge crossing for this potential condition extremely challenging. When considered in addition to the hydraulic complexity associated with expansion and contraction zones in this reach, suitability for a clear span bridge crossing is low. Geomorphic reach 7 has moderate suitability for a clear span bridge crossing. However, significant historical channel change in geomorphic reach 7 and the presence of complex channel forms and tributary interactions would make design of a clear span bridge for this location difficult as well. Based on preliminary analysis of potential meander cutoff paths from the Horseshoe Bend through geomorphic reach 6 and historical channel migration in geomorphic reach 7, a proposed clear span bridge crossing in geomorphic reach 7 should be cited either upstream of the confluence with Clear Creek or near the downstream extent of the Study Area. Geomorphic reach 4 clearly has the highest suitability for a clear span bridge. It has experienced very limited historical migration, and the geomorphic conditions in the reach are simple and fairly predictable. It should be relatively straightforward to avoid physical impacts on the Little Miami River and its floodplain in this location by accounting for the average annual migration rate in the design of the clear span bridge.

TABLE 4
Geomorphic reach suitability for clear span bridge crossing

Geomorphic Reach	Historical Morphology	1932-2007 Average Annual Migration Rate[1] (ft/yr)	Hydraulics	Sediment Transport	Crossing Suitability	Other Considerations
4	Limited Migration	2.4	High Velocity; Uniform Flow Vectors	Uniform Shear Patterns	High	Higher stability in middle of reach
5	Extensive Migration	15.3	Wide Velocity Range; Complex Flow Vectors	Complex Shear Patterns	Low	Secondary channels and tributaries add to potential instability
6	Moderate Migration	7.2	High Velocity; Uniform Flow Vectors with Contraction and Expansion	Uniform Shear Patterns	Low	High potential for meander cutoff in upstream geomorphic reach could cause major change in this reach
7	Moderate-high Migration	10.4	Wide Velocity Range; Complex Flow Vectors	Complex Shear Patterns	Moderate	Tributary confluence adds to potential instability due to sediment delivery and potential for high short-term migration rates

[1] Calculated as the average of left and right bank long-term average annual migration rates at the location of maximum long-term migration as summarized in Table 3

The Little Miami River exhibits relatively natural geomorphic processes (e.g. erosion, deposition, vegetation succession, etc.) in the Study Area that create and maintain intact aquatic and riparian habitats. However, some habitat degradation has occurred in the Little Miami River near the Study Area, and certain restoration and enhancement measures could improve overall river corridor habitat conditions. The biggest river corridor improvement would likely come from removing existing riprap and other hard, engineered bank protection measures and replacing them with either natural channel banks or bioengineered bank protection. The existing bank protection measures have eliminated the important habitat-creating process of bank erosion and have unnaturally deflected flow energy, possibly causing accelerated rates of bank erosion downstream. The channel also appears to be adjusting to a potentially increased rate of incision, as evidenced by the exposed root networks of mature trees throughout the Study Area. This could be associated with sediment starvation due to trapping by the two upstream reservoirs. Restoration measures such as sediment augmentation could be considered to offset this apparently ongoing adjustment. However, additional assessment of sediment transport in the Little Miami River would be required to determine the potential value of this possible restoration measure. Additional restoration measures could include removal of exotic vegetation and replacement with native species and establishment of riparian floodplain habitat buffer zones.

The second phase of this evaluation is intended to refine and calibrate the hydraulic and sediment transport models using high flow measurements and observations completed during the winter of 2008 / 2009 for the geomorphic reaches that have not been eliminated from consideration as a clear span bridge crossing location. The refined models will be used to conduct more detailed morphologic assessments of suitable geomorphic reaches to guide clear span bridge site selection within each geomorphic reach. This will likely include evaluations of likely meander cutoff paths and their influence on geomorphic reaches 5, 6, and 7, influences of tributary channels, and implications of finer-scale hydraulic and sediment transport characteristics.

References

Environmental Systems Research Institute. 2007. ArcInfo 9.2 [software]. Redlands, California: Environmental Systems Research Institute.

H.C. Nutting. 2008. Geotechnical archive review and data submittal Eastern Corridor Segment II/III Cincinnati/Newtown, Hamilton County, Ohio. Technical Memorandum provided to ENTRAN 10/14/08.

Koltun, G.F. 2003. Techniques for estimating flood-peak discharges of rural, unregulated streams in Ohio. Water-resources Investigations Report 03-4164, second edition. U.S. Geological Survey prepared in cooperation with the Ohio Department of Transportation, and the U.S. Department of Transportation, Federal Highway Administration.

Schiefer, M. C. 2002. Bulletin 47: Basin descriptions and flow characteristics of Ohio streams. Ohio Department of Natural Resources, Division of Water, Columbus, Ohio.

Stantec. 2008. Eastern Corridor Priority Part B Work – Segment II/III Little Miami River Sediment Sampling. Technical Memorandum provided to CH2M HILL 12/5/08.

United States Army Corps of Engineers (USACE). 2008a. http://www.lrl.usace.army.mil/wc/article.asp?id=11&MyCategory=74

United States Army Corps of Engineers (USACE). 2008b. http://www.lrl.usace.army.mil/wc/article.asp?id=28&MyCategory=73

Appendix A – Geomorphic Reconnaissance Photos

Exposed mature tree roots in geomorphic reach 4 illustrate dynamic nature of the Little Miami River and potential accelerated rate of incision in the Study Area.

Right bank point bar downstream of the railroad bridge showing downstream fining and relatively large size of fluvially transported sediment in the Study Area. This bar also shows riparian vegetation with a diverse age structure, which is further evidence of regular channel change.

Relatively large, fluvially transported channel bar sediments in geomorphic reach 1 are evidence of the high energy of peak discharges in the Study Area.

Relatively clear secondary channel shows regularity of overbank flows in the Study Area.

Expansive clear point bar along the inside of the Horseshoe Bend in geomorphic reach 5 clearly illustrates the highly dynamic nature of this reach.

Eroding banks in geomorphic reach 7 show the nature of ongoing channel change in the Study Area and the fine-grained sediment composition of the floodplain and channel banks.

Failed bank protection along the outside of Horseshoe Bend highlights the unsuitability of geomorphic reach 5 for a clear span bridge crossing.